AMERICAN SOCIETY FOR MICROBIOLOGY | Journal of Bacteriology®

RESEARCH ARTICLE

Recruitment of the TolA Protein to Cell Constriction Sites in *Escherichia coli* via Three Separate Mechanisms, and a Critical Role for FtsWI Activity in Recruitment of both TolA and TolQ

Cynthia A. Hale,[a] Logan Persons,[a] Piet A. J. de Boer[a]

[a]Department of Molecular Biology and Microbiology, School of Medicine, Case Western Reserve University, Cleveland, Ohio, USA

ABSTRACT The Tol-Pal system of Gram-negative bacteria helps maintain the integrity of the cell envelope and ensures that invagination of the envelope layers during cell fission occurs in a well-coordinated manner. In *Escherichia coli*, the five Tol-Pal proteins (TolQ, -R, -A, and -B and Pal) accumulate at cell constriction sites in a manner that normally requires the activity of the cell constriction initiation protein FtsN. While septal recruitment of TolR, TolB, and Pal also requires the presence of TolQ and/or TolA, the latter two can recognize constriction sites independently of the other system proteins. What attracts TolQ or TolA to these sites is unclear. We show that FtsN indirectly attracts both proteins and that PBP1A, PBP1B, and CpoB are dispensable for their septal recruitment. However, the β-lactam aztreonam readily interferes with the septal accumulation of both TolQ and TolA, indicating that FtsN-stimulated production of septal peptidoglycan by the FtsWI synthase is critical to their recruitment. We also discovered that each of TolA's three domains can separately recognize division sites. Notably, the middle domain (TolAII) is responsible for directing TolA to constriction sites in the absence of other Tol-Pal proteins and CpoB, while recruitment of TolAI requires TolQ and that of TolAIII requires a combination of TolB, Pal, and CpoB. Additionally, we describe the construction and use of functional fluorescent sandwich fusions of the ZipA division protein, which should be more broadly valuable in future studies of the *E. coli* cell division machinery.

IMPORTANCE Cell division (cytokinesis) is a fundamental biological process that is incompletely understood for any organism. Division of bacterial cells relies on a ring-like machinery called the septal ring or divisome that assembles along the circumference of the mother cell at the site where constriction will eventually occur. In the well-studied bacterium *Escherichia coli*, this machinery contains over 30 distinct proteins. We studied how two such proteins, TolA and TolQ, which also play a role in maintaining the integrity of the outer membrane, are recruited to the machinery. We find that TolA can be recruited by three separate mechanisms and that both proteins rely on the activity of a well-studied cell division enzyme for their recruitment.

KEYWORDS Cell division, ZipA, FtsN, Tol-Pal

The process of cell fission (cytokinesis, division, constriction, and septation) in Gram-negative bacteria involves coordinated modifications to the cell envelope layers at the site of constriction. These include (i) invagination of the inner membrane (IM), (ii) production of an inward growing annulus of septal peptidoglycan (sPG), (iii) splitting of the outer portion of the sPG annulus into the two PG layers that will define the new cell poles, and (iv) invagination of the outer membrane (OM) into the space created by sPG splitting. All these modifications are executed in a coordinated fashion by components of a transenvelope ring-like cytokinetic machinery called the divisome or septal ring (1, 2).

Editor Yves V. Brun, Université de Montréal

Address correspondence to Piet A. J. de Boer, pad5@case.edu.

The authors declare no conflict of interest.

Received 10 September 2021
Accepted 4 November 2021
Accepted manuscript posted online 8 November 2021
Published 18 January 2022

The septal ring (SR) in *E. coli* includes over 30 distinct protein components. Ten of these (FtsA, -B, -I, -K, -L, -N, -Q, -W, and -Z and ZipA) are normally essential for both cell fission and survival and can be considered the core SR components. The lack of any one core protein prevents steps i and/or ii noted above and results in the formation of long and smooth multinucleoid filamentous cells that eventually die (1, 2). Formation of the SR starts with the accumulation of cytoplasmic FtsZ and its membrane-associated interaction partners FtsA and ZipA at the future site of constriction to form an intermediate dynamic assembly, called the FtsZ ring or Z-ring (1, 3). Within this assembly, treadmilling polymers of FtsZ move along the inner circumference of the cell as FtsA and ZipA hold them closely apposed to the inner surface of the IM (4, 5). The Z-ring then attracts FtsEX and FtsK, followed by recruitment of FtsBLQ, a complex of the FtsQ, -L, and -B proteins. FtsBLQ then attracts the sPG synthase FtsWI consisting of the peptidoglycan glycosyltransferase FtsW and the PG transpeptidase FtsI (PBP3), a class B monofunctional penicillin-binding protein (1, 2, 6). Finally, maturation to a constriction-competent apparatus requires FtsN, a bitopic IM protein that is normally required to trigger and sustain the constriction process and whose accumulation at the SR is significantly reinforced by the constriction process itself (1, 2, 7, 8).

FtsN acts on either side of the IM to indirectly stimulate the conversion of FtsWI from an inactive ("off") to active ("on") sPG synthase and is proposed to do so by affecting the conformational states (from off to on) of FtsA in the cytoplasm and the FtsBLQ subcomplex in the periplasm (8–12). Evidence for this has come in part from the isolation of mutant "superfission" (SF) variants of FtsA, -B, -I, -L, and -W that bypass the requirement for FtsN to various degrees (8, 9, 13–15).

Besides FtsWI, which is dedicated to producing septal PG, the bifunctional class A PBP's PBP1B and PBP1A also contribute to sPG synthesis during cell constriction in addition to their roles in cylindrical PG synthesis during cell elongation (16–18). Neither PBP1A nor 1B is individually essential for cell survival, but the absence of both leads to cell lysis (19, 20). Biochemical evidence indicates that FtsN also interacts with PBP1B and modestly stimulates its activity (18, 21, 22).

Like PBP1A and PBP1B, many other noncore SR proteins that are individually dispensable for cell survival, *per se*, nevertheless play significant roles in the cell fission process, in particular at steps iii (sPG splitting) and iv (OM invagination) (1, 2).

The Tol-Pal system constitutes one intriguing subset of such SR proteins (23, 24). Tol-Pal consists of the polytopic IM-protein TolQ, the bitopic (N-in) IM-proteins TolR and TolA, the periplasmic protein TolB, and the lipoprotein Pal (25, 26) (Fig. 1A). The latter is an abundant OM species that binds stem peptides of the underlying PG layer in a reversible manner (27–29). The system is highly conserved among Gram-negative bacteria (30, 31) and is essential to the survival of some but not all species. While it is not essential to the viability of *E. coli* K-12, cells lacking a functional Tol-Pal system display a variety of phenotypes (25, 26). These include reduced OM barrier function and increased sensitivity to detergents and other antibacterials (23, 24, 32–35), the prodigious release of large OM vesicles from cell division sites and cell poles (23, 33, 36), and inefficient OM invagination and sPG splitting during cell fission, causing the formation of cell chains especially in low-osmotic medium (23, 37–41).

TolQ, TolR, and TolA form a complex in the IM, where TolQ and R use proton motive force (pmf) to "energize" TolA (42–47). TolA contains 421 residues and 3 domains called TolAI (TolA$^{1\text{-}42}$), TolAII (TolA$^{48\text{-}310}$), and TolAIII (TolA$^{314\text{-}421}$), the latter two of which reside in the periplasm (48) (Fig. 2A). TolAI includes the transmembrane (TM) anchor (TolA$^{14\text{-}34}$), which interacts with both TolQ and TolR within the IM bilayer (49–51). TolAII is almost entirely α-helical, likely folds into a three-stranded coiled-coil, and forms a stalk-like structure that places TolAIII roughly equidistant ($\sim$10 nm) to the IM and OM (48, 52, 53). TolAIII is a globular domain with a well-defined structure and binds TolB (53–60).

TolQ and R form a proton channel and belong to a larger family of proton/ion conductors that drive a variety of dynamic envelope processes in bacteria (61–63). In the case of the Tol-Pal system, proton flow through the TolQ/R channel is proposed to be

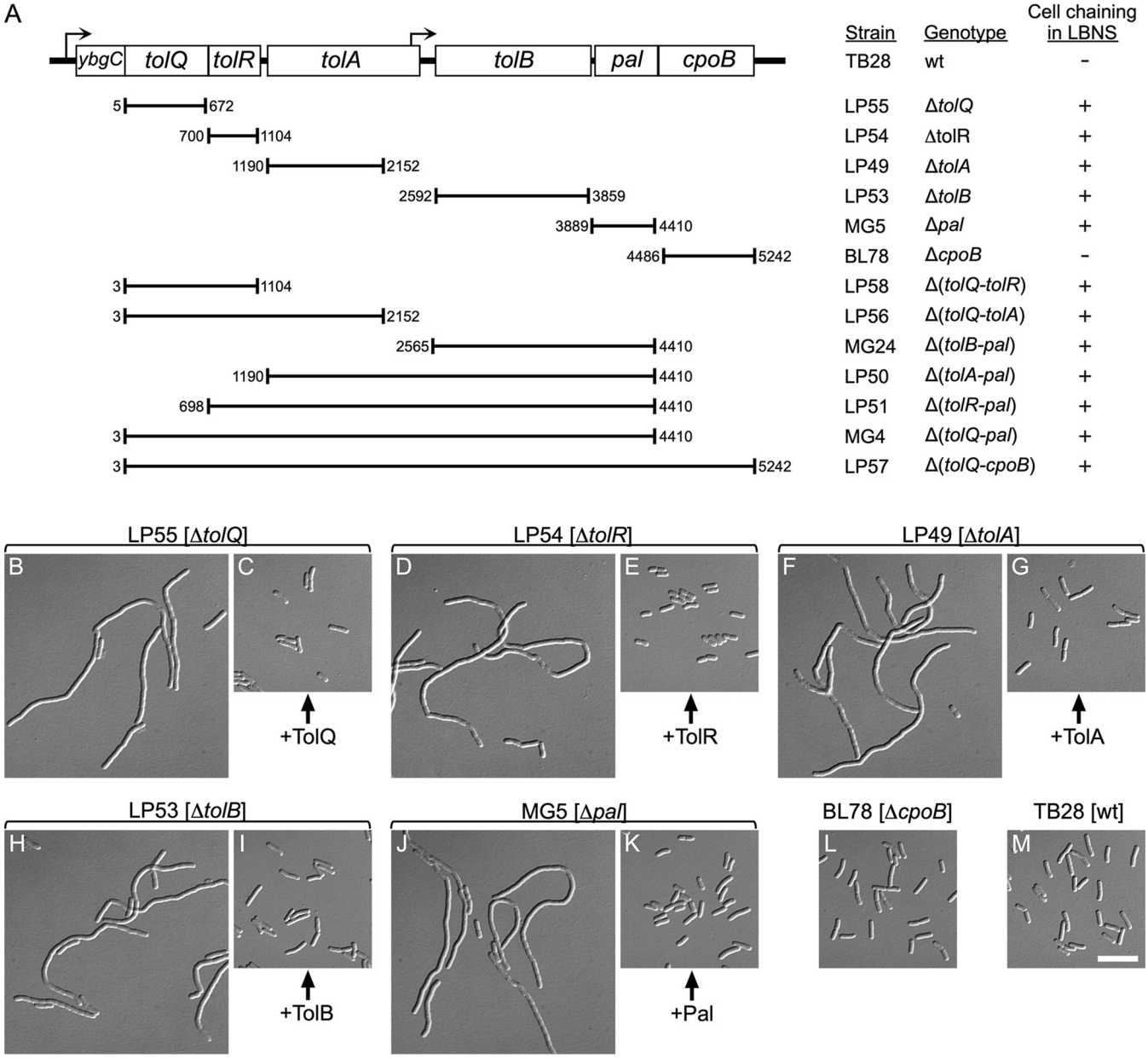

FIG 1 Strains lacking one or more genes of the *tolQ-cpoB* cluster. (A) The organization of *tol-pal* and *cpoB* genes on the *E. coli* chromosome is depicted. Hooked arrows indicate the direction of transcription and the locations of predicted promoters (117). Chromosomal fragments that were replaced with *aph* (kanamycin resistance) to yield the various deletion derivatives of strain TB28 (wt) are indicated below the schematic. Numbers correspond to the first and last base pairs of replaced fragments, counting from the start of *tolQ*. Columns on the right list corresponding strain names, genotypes, and whether the cells formed chains in LBNS medium (+) or displayed a normal division phenotype (−). (B to M) Cell chaining caused by nonpolar deletions in *tolQ*, *tolA*, *tolR*, *tolB*, or *pal*. Differential interference contrast (DIC) images of chemically fixed cells of strains LP55 (Δ*tolQ*) (B and C), LP54 (Δ*tolR*) (D and E), LP49 (Δ*tolA*) (F and G), LP53 (Δ*tolB*) (H and I), MG5 (Δ*pal*) (J and K), BL78 (Δ*cpoB*) (L), and TB28 (wt) (M). Strains carried pLP146 (P_{BAD}::*tolQ*) (C), pLP225 (P_{BAD}::*tolR*) (E), pCH555 (P_{BAD}::*tolA*) (G), pMG45 (P_{BAD}::*tolB*) (I), pCH525 (P_{BAD}::*pal*) (K), or the vector control pBAD33 (P_{BAD}::) (all others). Cultures were grown to density overnight in regular LB (0.5% NaCl), diluted 200-fold in LBNS (no added NaCl) with 0.05% arabinose, and further incubated for ~5 mass doublings to optical density at 600 nm (OD_{600}) of 0.6 to 0.7 before fixation. Bar equals 10 μm.

coupled to a conformational change in TolA, likely within TolAII more specifically (43), that allows TolAIII to be chemically cross-linked *in vivo* to Pal or a Pal-containing complex (24, 42, 46, 64, 65). Thus, "energized" TolA may adopt an extended conformation, allowing it to reach through the PG mesh toward the OM (23, 42). Although some Pal can be recovered from cells with TolA in cross-linked complexes, two-hybrid assays and biochemical analyses of purified proteins indicate that TolAIII and Pal do not interact directly (57, 58) (our unpublished results). While it is difficult to exclude that a Pal-binding

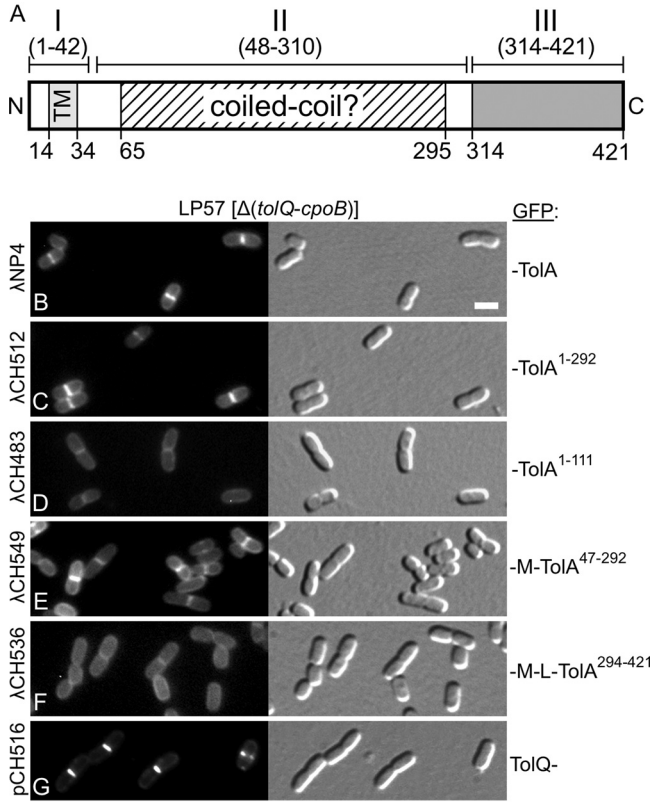

FIG 2 Recruitment of TolA$^{47-292}$ (~TolAII) to division sites in the absence of other Tol-Pal components. (A) Schematic showing domain organization and other features of the *E. coli* TolA protein. Domain TolAII (TolA$^{48-310}$) is linked to domains TolAI (TolA$^{1-42}$) and TolAIII (TolA$^{314-421}$) by stretches of five and three glycine residues, respectively. TolAI includes the cytoplasmic N-terminal peptide (TolA$^{1-13}$), the transmembrane helix (TM, TolA$^{14-34}$), and some periplasmic residues (TolA$^{35-42}$). TolAII is dominated by a long stretch of residues (TolA$^{65-295}$) with a high propensity to adopt the α-helical coiled-coil fold as predicted with Paircoil2 (*P* score cutoff = 0.03) (118). TolAIII (TolA$^{314-421}$) is a well-defined C-terminal periplasmic domain of known structure (53–55). (B to G) Fluorescence (left) and DIC (right) images of live LP57 (Δ[*tolQ-cpoB*]) cells producing GFP fusions to full-length TolA$^{1-421}$ (TolAI+II+III) (B), TolA$^{1-292}$ (~TolAI+II) (C), TolA$^{1-111}$ (~TolAI) (D), MalF$^{2-39}$-TolA$^{47-292}$ (~TolAII) (E), MalF$^{2-39}$-RodZ$^{139-255}$-TolA$^{294-421}$ (~TolAIII) (F), or full-length TolQ (G). MalF$^{2-39}$ (M) includes the first transmembrane helix (MalF$^{19-35}$) of the MalF protein (89), and RodZ$^{139-255}$ (L) corresponds to the periplasmic linker that connects the TM and C-terminal domains of the RodZ protein (90). Fusions were encoded on lysogenic phages λNP4 (P$_{lac}$::*gfp-tolA*) (B), λCH512 (P$_{lac}$::*gfp-tolA*$^{1-292}$) (C), λCH483 (P$_{lac}$::*gfp-tolA*$^{1-111}$) (D), λCH549 (P$_{lac}$::*gfp-malF*$^{2-39}$-*tolA*$^{47-292}$) (E), or λCH536 (P$_{lac}$::*gfp-malF*$^{2-39}$-*rodZ*$^{139-255}$-*tolA*$^{294-421}$) (F) or on plasmid pCH516 (P$_{lac}$::*tolQ-gfp*) (G). Cells were grown for ~3.5 mass doublings to OD$_{600}$ = 0.5 to 0.6 in M9-maltose medium with 37 μM (B to F) or 5 μM (G) IPTG. Bar equals 2 μm.

interface might only present itself on the "energized" form of TolA, it is more likely that the apparent TolA-Pal interaction *in vivo* is mediated by bridging molecules. One obvious candidate for such an intermediary is the TolB protein (57, 58).

TolB is fully periplasmic and has an N-terminal globular domain that binds TolAIII and a C-terminal β-propeller domain that binds Pal (57, 58, 60, 66, 67). TolB-bound Pal cannot also bind PG (64, 68, 69). In turn, binding of Pal to the β-propeller of TolB allosterically reduces the affinity of TolB for TolAIII *in vitro*, while the capture of the N terminus of TolB by TolAIII likely reduces the affinity of TolB for Pal in an opposite manner (58). This predicts that, *in vivo*, PG-free Pal weakens the TolB-TolA interaction (58, 70) and/or that TolA reduces the interaction between TolB and Pal (40, 60, 71).

Although their half-lives are probably short, heterotrimeric TolA-TolB-Pal complexes are still sufficiently stable to be readily detectible *in vitro* (58). This is of interest considering our previous proposal that the Tol-Pal system helps invaginate the OM by establishing waves of transient OM-PG connections (via direct Pal-PG interactions) and/or of OM-IM connections (via direct or indirect Pal-TolA interactions) that trail the core SR as

it constricts the IM and forms the two new polar PG caps (23). Even if TolA and Pal do not interact directly, transient TolA-TolB-Pal ternary complexes could play a significant role in promoting OM invagination during cell fission. Alternatively, Tol-Pal-mediated OM invagination could be primarily driven by transient Pal-PG interactions within the SR, where repeated cycles of Pal-PG binding and unbinding are promoted by the interactions of energized TolA with TolB-Pal (freeing Pal to bind PG) and of free TolB with Pal-PG (freeing PG, and forming TolB-Pal again) (40, 60, 71).

The *E. coli tol-pal* locus comprises 7 genes (*ybgC*, *tolQ*, *tolR*, *tolA*, *tolB*, *pal*, and *cpoB*), (co)transcribed from promoters upstream of *ybgC* and *tolB* (72) (Fig. 1A). YbgC is a cytoplasmic thioesterase with no obvious role in cell division or other Tol-Pal functions (73–75). CpoB (YbgF) is completely periplasmic and contains an N-terminal coiled-coil domain and a C-terminal TPR-repeat domain (72, 76, 77). CpoB also plays either no role or only a minor role in classical Tol-Pal functions (72, 78). However, CpoB does bind TolA (57, 76), and both proteins can form a higher-order complex with PBP1B (77, 78). Moreover, within this complex, CpoB and TolA modulate the murein glycosyltransferase (GT) and transpeptidase (TP) activities of PBP1B in a manner that is, at least in part, dependent on the energization status of TolA and, hence, on TolQ and TolR functions (78).

Like the five Tol-Pal proteins (23), CpoB accumulates at the SR at or shortly after the initiation of cell constriction (78). What attracts these proteins to sites of division is an interesting question. We previously determined that accumulation of TolR or Pal at the SR requires the presence of at least one of the other four Tol-Pal proteins but that both TolQ and TolA can localize to division sites independently of other Tol-Pal components (23). What attracts TolQ or TolA to these sites is unclear. We found here that FtsN attracts both proteins to the SR in an indirect fashion and that PBP1A, PBP1B, and CpoB are dispensable for their septal recruitment. However, the β-lactam aztreonam readily interferes with the septal accumulation of both TolQ and TolA, indicating that FtsN-stimulated production of sPG by the FtsWI synthase is normally critical to their recruitment.

To better understand how the TolA protein accumulates at sites of cell constriction, we also studied what part of the protein is responsible for this localization. Notably, the results show that each of the three TolA domains can contribute to septal localization, but that they do so under different requirements. We found that domain TolAII is both required and sufficient for septal accumulation of TolA in the absence of the other four Tol-Pal proteins and CpoB. In addition, domain TolAI is recruited to division septa provided the cells produce TolQ, whereas TolAIII is recruited to septa provided cells produce TolB, Pal, and CpoB.

Finally, we describe the construction of fluorescent variants of the ZipA protein that retain essential ZipA function. These variants were used in some of the experiments described here and should be more broadly valuable in future studies of the *E. coli* cell division machinery.

RESULTS

A set of isogenic strains that lack one or more of the five Tol-Pal components and/or CpoB. *E. coli* mutants of various genetic backgrounds that lack TolQ, TolR, TolA, or Pal are known to display a cell chaining phenotype in low-osmotic medium (23, 37, 38). To better compare the phenotypes of such mutants and those associated with loss of TolB or CpoB, we generated a set of isogenic derivatives of strain TB28 (wild type [wt]) in which one of each of these components is missing (Fig. 1A). Strain MG5 (Δ*pal*) was described before (23). Strains BL78 (Δ*cpoB*) and LP49 (Δ*tolA*) were generated by λred-mediated recombineering, and LP53 (Δ*tolB*), LP54 (Δ*tolR*), and LP55 (Δ*tolQ*) were obtained by transduction of the corresponding mutation from the Keio collection (79) into TB28.

As anticipated, LP55 (Δ*tolQ*), LP54 (Δ*tolR*), LP49 (Δ*tolA*), and MG5 (Δ*pal*) cells formed distinct chains when grown in LB medium lacking added NaCl (LB no salt [LBNS]) (Fig. 1B, D, F, and J). In addition, LP53 (Δ*tolB*) cells formed similar chains in this medium (Fig. 1H).

TABLE 1 Localization of TolA derivatives in the absence of other Tol-Pal proteins and CpoB[a]

GFP fusion[b]			% of cells with accumulation[c]			
Phage	Residues	TolA domain(s)	+ +	+ −	− −	*n*[d]
λNP4	-TolA$^{1-421}$	I+II+III	49	11	40	191
λDE2	-TolA$^{1-328}$	I+II	35	12	53	321
λCH512	-TolA$^{1-292}$	I+II'	48	10	42	503
λCH483	-TolA$^{1-111}$	I	4	12	84	348
λDE3	-TolA$^{1-60}$	I	1	5	94	364
λCH509	-MalF$^{2-39}$-TolA$^{47-421}$	II+III	35	13	52	372
λCH510	-MalF$^{2-39}$-TolA$^{47-328}$	II	34	15	51	282
λCH549	-MalF$^{2-39}$-TolA$^{47-292}$	II'	34	14	52	228
λCH536	-MalF$^{2-39}$-RodZ$^{139-255}$-TolA$^{294-421}$	III	0	1	99	528

[a]LP57(Δ[*tolQ-cpoB*]) cells lysogenic for the indicated phage were grown for ~3.5 mass doublings to OD_{600} = 0.5 to 0.6 in M9-maltose medium with IPTG and imaged live. IPTG was used at 25 or 37 μM for each lysogen, and the results from both conditions were combined.

[b]Indicated are the name of the lysogenic phage encoding the fusion under the control of the *lac* regulatory region, the TolA residues encoded, and the presence of intact TolAI (TolA$^{1-42}$), TolAII (TolA$^{48-310}$), and/or TolAIII (TolA$^{314-421}$) domains in the fusion (48). II' indicates that the encoded TolAII domain is slightly truncated at its C-terminal end. GFP is N terminal in all cases. MalF$^{2-39}$ includes the first transmembrane helix of MalF (MalF$^{19-35}$) (89). RodZ$^{139-255}$ corresponds to the periplasmic linker domain of the RodZ protein (90).

[c]Percentage of cells in which the GFP fusion accumulated strongly (+ +) or weakly (+ −) at sites of cell constriction or appeared evenly distributed along the periphery of cells (− −).

[d]Number of cells scored.

Importantly, cell chaining in LBNS by each of the five mutant strains could be completely corrected by the expression of the missing gene from a plasmid (Fig. 1C, E, G, I, and K). Thus, if any of the deletions in these strains caused polarity, the effects on expression of surrounding genes were too weak to result in cell chaining by themselves.

We also used recombineering to generate several strains deleted for two or more genes in the *tolQ-cpoB* cluster, and each displayed the cell chaining phenotype in LBNS also observed with the single gene deletions described above (Fig. 1A). Moreover, in each single- or multiple-gene *tol-pal* mutant, the cell chaining was largely suppressed by growth in regular LB (containing 0.5 or 1.0% NaCl) or in M9 minimal medium as noted before for some of the deletion mutants (23). We infer that the lack of one or more of the five Tol-Pal proteins in *E. coli* results in a similar cell chaining division defect, which is consistent with observations from various subsets of *tol-pal* mutants of *Vibrio cholerae* (80), *Pseudomonas putida* (81), *Erwinia chrysanthemi* (82), *Caulobacter crescentus* (24), *Pseudomonas aeruginosa* (83), *Shewanella oneidensis* (84), and *E. coli* (40, 41).

In contrast, BL78 (Δ*cpoB*) cells showed no overt division defects in LBNS (Fig. 1L), which correlates with the absence of other Tol-Pal-associated phenotypes in cells lacking CpoB (72, 78, 85).

TolA or TolQ accumulation at division sites does not require the other four Tol-Pal proteins, CpoB, PBP1A, or PBP1B. We previously showed that a functional fluorescent fusion of green fluorescent protein (GFP) to full-length TolA (GFP-TolA$^{1-421}$ or GFP-TolA) accumulated at sites of cell constriction and that it does so even when TolQ, TolR, TolB, and Pal are missing (23). Similarly, a fusion of full-length TolQ to GFP (TolQ$^{1-230}$-GFP or TolQ-GFP) accumulated at constriction sites independently of TolA, TolR, TolB, and Pal (23). The finding that TolA interacts with CpoB (57, 76, 78) raised the possibility that the latter played a role in the recruitment of TolA to constriction sites. To test this, we examined the location of GFP-TolA in cells of strain LP57 (Δ*tolQ-cpoB*), which lacks the consecutive *tolQ*, *tolR*, *tolA*, *tolB*, *pal*, and *cpoB* genes (Fig. 1A). The fusion was encoded on chromosomally integrated lysogenic phage λNP4 (P_{lac}::*gfp-tolA*) with its production placed under transcriptional control of the *lac* regulatory region. Cells were grown in M9-maltose medium, a condition that suppresses cell chaining, and then imaged by fluorescence and differential interference (DIC) microscopy. GFP-TolA accumulated at constriction sites in LP57 (λNP4) (Δ*tolQ-cpoB*[P_{lac}::*gfp-tolA*]) cells (Fig. 2B and Table 1), implying that CpoB is not required for TolA localization.

Like GFP-TolA (23), the TolQ-GFP fusion retained function as based on its ability to suppress cell chaining and detergent sensitivity of LP55 (Δ*tolQ*) cells (see Fig. S1 in the supplemental material; also data not shown). In addition, TolQ-GFP still accumulated sharply at constriction sites in LP57/pCH516 (Δ*tolQ-cpoB*/P_{lac}::*tolQ-gfp*) cells (Fig. 2G). Thus, neither any of the other four Tol-Pal proteins nor CpoB is required for the recruitment of TolA or TolQ to sites of cell constriction.

Given the evidence that TolA can interact with PBP1B *in vitro* and *in vivo* (78) and that PBP1B itself accumulates at cell fission sites (86), we also examined the localization of GFP-TolA and TolQ-GFP in derivatives of LP57 that additionally lacked PBP1B or PBP1A as a control. Cells lacking both PBP1B and a functional Tol-Pal system are prone to lysis and grow poorly (87). Accordingly, strain CH237 (Δ*tolQ-cpoB* Δ*ponB*) grew poorly in both rich and minimal medium, and cultures contained a significant amount of cell debris. Even so, GFP-TolA and TolQ-GFP still accumulated at constriction sites of both CH236 (Δ*tolQ-cpoB* Δ*ponA*) and CH237 (Δ*tolQ-cpoB* Δ*ponB*) cells (Fig. S2), implying that PBP1A and PBP1B are also dispensable for the recruitment of TolA or TolQ to sites of cell constriction.

TolA domain II (TolAII) accumulates at division sites in the absence of Tol-Pal and CpoB proteins. To identify the part(s) of TolA involved in directing the protein to division sites, we studied derivatives of GFP-TolA in which one or two of the three TolA domains were missing or replaced with part of an unrelated protein. We first constructed a set of derivatives of the moderate-copy-number plasmid pNP4 (P_{lac}::*gfp-tolA*) (23) and then crossed each with λNT5 to obtain a corresponding set of lysogenic phages (88). Western blot analyses indicated that none of the GFP-TolA derivatives used in this study were subject to excessive degradation (Fig. S3). Still, only the GFP fusion to full-length TolA was able to correct the chaining phenotype of LP49 (Δ*tolA*) cells in LBNS medium (Table S1), which parallels previous findings that each of TolA's three domains is required to maintain OM integrity (49, 50).

The phages were integrated into the chromosome of LP57 (Δ*tolQ-cpoB*) and resulting lysogens were examined by microscopy as above. Fusions encoded by λDE2 (GFP-$TolA^{1-328}$) or λCH512 (GFP-$TolA^{1-292}$) lack most or all of TolAIII (Fig. 2A). They still accumulated at division sites, however, showing that this domain of TolA is not required for its localization (Fig. 2C; Table 1).

In contrast, fusions lacking both TolAII and III, encoded by λCH483 (GFP-$TolA^{1–111}$) or λDE3 (GFP-$TolA^{1–60}$), no longer accumulated at division sites but appeared evenly dispersed along the membrane (Fig. 2D, Fig. 3C, and Table 1). These results implied that TolAI is not sufficient, and also suggested that TolAII is required, for TolA to recognize division sites in LP57 (Δ*tolQ-cpoB*) cells. Accordingly, fusions in which TolAI had been replaced with a portion of the MalF protein (89), which includes its N-terminal cytoplasmic residues ($MalF^{2-18}$) and first transmembrane helix ($MalF^{19-35}$, TM1), accumulated at division sites, provided they contained TolAII (Fig. 2E; Table 1). Septal localization patterns of GFP-$MalF^{2-39}$-$TolA^{47-328}$ and GFP-$MalF^{2-39}$-$TolA^{47-292}$ (GFP-M-TolAII for short) were similar to that of GFP-$MalF^{2-39}$-$TolA^{47-421}$ (Table 1), reinforcing the notion that TolAIII does not contribute to septal localization of TolA in LP57 (Δ*tolQ-cpoB*) cells. In contrast, substitution of the TolAII portion in GFP-$MalF^{2-39}$-$TolA^{47-421}$ with the periplasmic linker domain of the RodZ protein (90) yielded a fusion encoded by λCH536 (GFP-$MalF^{2-39}$-$RodZ^{139-255}$-$TolA^{294-421}$ or GFP-M-L-TolAIII) that appeared evenly distributed along the periphery of cells but failed to accumulate at sites of constriction (Fig. 2F; Table 1). We conclude that TolAII represents or contains a septal localization determinant that allows TolA to accumulate at division sites independently of the other Tol-Pal components and CpoB.

TolQ-dependent recruitment of TolA to division sites mediated by domain I (TolAI). As discussed above, fusions lacking the TolAII domain failed to accumulate at division sites in cells of strain LP57 (Δ*tolQ-cpoB*) (Fig. 2; Table 1). However, several of these fusions did show such accumulation in cells of strain LP49 (Δ*tolA*) that only lack chromosomally encoded TolA (Fig. S4; Table S1). This included the fusions GFP-$TolA^{1-111}$ (Fig. S4D) and GFP-$TolA^{1-60}$ (Fig. 3A; Fig. S4E), which bear an intact TolAI domain but

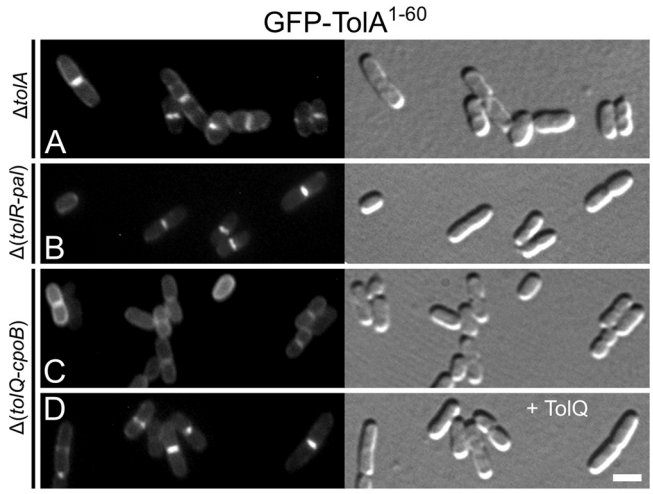

FIG 3 TolQ-dependent recruitment of TolAI (TolA$^{1-60}$) to division sites. Fluorescence (left) and DIC (right) images of lysogenic derivatives of strains LP49 (Δ*tolA*) (A), LP51 (Δ[*tolR-pal*]) (B), and LP57 (Δ[*tolQ-cpoB*]) (C and D), carrying λDE3 (P_{lac}::*gfp-tolA*$^{1-60}$) integrated in the chromosome. The cells in panel D also harbored plasmid pLP146 (P_{BAD}::*tolQ*). Cells were grown for ~3.5 mass doublings to OD_{600} = 0.5 to 0.6 in M9-maltose medium with 37 μM IPTG and either no (A to C) or 0.02% (D) arabinose and were imaged live. Bar equals 2 μm.

lack TolAII and TolAIII. These results suggested that TolAI can recognize division sites independently of TolAII but in a manner that requires one or more of the proteins that are absent in LP57 (Δ*tolQ-cpoB*). To assess the septal localization requirements of TolAI, we examined the localization patterns of GFP-TolA$^{1-60}$ (GFP-TolAI) in several additional strains (Fig. 3; Table 2). This showed that the fusion accumulated at division sites in LP49 (Δ*tolA*), LP50 (Δ*tolA-pal*), and LP51 (Δ*tolR-pal*) cells (Fig. 3A and B; Table 2) while it failed to do so in both LP57 (Δ*tolQ-cpoB*) and LP56 (Δ*tolQ-tolA*) cells (Fig. 3C; Table 2). Thus, septal localization of GFP-TolA$^{1-60}$ correlated precisely with retention of an intact *tolQ* gene in these deletion strains. Accordingly, production of TolQ from plasmid pLP146 (P_{BAD}::*tolQ*) or pLP147 (P_{BAD}::*tolQR*) resulted in the accumulation of GFP-TolA$^{1-60}$ at division sites in LP57(λDE3) cells (Fig. 3D; Table 2). In contrast, the production of just the TolR protein from pLP225 (P_{BAD}::*tolR*) was ineffective in causing septal localization of GFP-TolA$^{1-60}$ in these cells or in cells of strain LP56(λDE3)/pLP225 that, besides full-length TolA, only lack the TolQ protein (Table 2).

We conclude that TolQ is required to direct TolAI to division sites. In comparison, none of the other Tol-Pal components (TolR, TolB, and Pal) or CpoB by themselves or in combination appeared to direct the localization of TolAI. A role for TolQ in the recruitment of TolAI is nicely consistent with the findings that TolQ itself accumulates at constriction sites independently of the other Tol-Pal proteins and CpoB (Fig. 2G) (23), and that TolQ and TolA interact via their transmembrane domains (49, 50).

Recruitment of TolA to division sites via TolAIII. Interesting localization behavior was also observed with the GFP-M-L-TolAIII (GFP-MalF$^{2-39}$-RodZ$^{139-255}$-TolA$^{294-421}$) fusion protein in which both domains I and II of TolA have been replaced. Like the GFP-TolAI fusions described above, this fusion did not accumulate at septal sites in LP57 (Δ*tolQ-cpoB*) cells (Fig. 2F, Table 1, and Table 3) but did do so in cells of strain LP49 (Δ*tolA*) (Fig. 4B, Fig. S4K, Table 3, and Table S1). Septal localization in the latter case was dependent on TolAIII because a version of the fusion lacking this domain (GFP-MalF$^{2-39}$-RodZ$^{139-255}$) distributed evenly along the membrane of cells instead (Fig. 4A; Table 3). Another GFP-M-L-TolAIII variant (GFP-MalF$^{2-39}$-ZipA$^{86-145}$-TolA$^{294-421}$), wherein the linker between the MalF and TolAIII domains was derived from ZipA (91) instead of RodZ, similarly accumulated at constrictions in LP49 (Δ*tolA*) cells (Fig. S4J). Interestingly, however, a variant lacking an extended linker altogether (GFP-MalF$^{2-39}$-TolA$^{294-421}$) failed to

TABLE 2 TolQ-dependent septal localization of GFP-TolA$^{1-60}$

	Host[a]			Plasmid		
Row	Name	Genotype	Still present[c]	Name	Genotype	Accumulation at septa[b]
1	LP49	Δ*tolA*	*tolQRB*, *pal*, *cpoB*			+
2	LP57	Δ(*tolQ-cpoB*)				−
3	LP50	Δ(*tolA-pal*)	*tolQR*, *cpoB*			+
4	LP51	Δ(*tolR-pal*)	*tolQ*, *cpoB*			+
5	LP56	Δ(*tolQ-tolA*)	*tolB*, *pal*, *cpoB*			−
6	LP56	Δ(*tolQ-tolA*)	*tolB*, *pal*, *cpoB*	pLP225	P_{BAD}::*tolR*	−
7	LP57	Δ(*tolQ-cpoB*)		pBAD33	P_{BAD}::	−
8	LP57	Δ(*tolQ-cpoB*)		pLP147	P_{BAD}::*tolQR*	+
9	LP57	Δ(*tolQ-cpoB*)		pLP146	P_{BAD}::*tolQ*	+
10	LP57	Δ(*tolQ-cpoB*)		pLP225	P_{BAD}::*tolR*	−

[a]Strains lysogenic for λDE3 (P_{lac}::*gfp-tolA*$^{1-60}$) and harboring the indicated plasmid (rows 6 to 10 only) were grown for ~3.5 mass doublings to OD_{600} = 0.5 to 0.6 in M9-maltose medium with 37 μM IPTG (all rows) and either no (rows 1 to 5) or 0.02% (rows 6 to 10) arabinose.
[b]GFP-TolA$^{1-60}$ distributed evenly along the periphery of cells (−) or accumulated at sites of cell constriction (+).
[c]Genes of the *tolQ-cpoB* cluster that are still present on the chromosome.

do so (Fig. S4I; Table S1). These results suggest that for TolAIII to be attracted to constriction sites in LP49 (Δ*tolA*) cells, it needs some freedom of movement to recognize recruiting molecules at these sites, perhaps because they reside some distance away from the IM.

To determine the septal localization requirements of TolAIII, we examined the localization patterns of GFP-M-L-TolAIII in other strains that lack one or more of the Tol-Pal proteins (Fig. 4 and 5; Table 3). The fusion still accumulated at constrictions in LP56 (Δ*tolQ-tolA*) cells (Fig. 4C), showing that TolQ and TolR are dispensable for this localization pattern. In contrast, the fusion failed to accumulate at division sites in strain LP50 (Δ*tolA-pal*) (Fig. 4D), indicating that TolB, Pal, and/or CpoB played a role in the recruitment of GFP-M-L-TolAIII to these sites.

We tested the requirements for these proteins in strain LP57 (Δ*tolQ-cpoB*), lysogenic for λCH536 (P_{lac}::*gfp-malF*$^{2-39}$-*rodZ*$^{139-255}$-*tolA*$^{294-421}$) and carrying one of several plasmids encoding *tolB*, *pal*, and/or *cpoB* under control of the *ara* regulatory region. Consistent with its localization in LP56(λCH536) cells (Fig. 4C), GFP-M-L-TolAIII

TABLE 3 Septal recruitment of TolAIII by TolB, Pal, and CpoB

	Host[a]			Plasmid		
Row	Name	Genotype	Still present[c]	Name	Genotype	Accumulation at septa[b]
1	TB28	wt	*tolQRAB*, *pal*, *cpoB*			+
2	LP49	Δ*tolA*	*tolQRB*, *pal*, *cpoB*			+
3	LP56	Δ(*tolQ-tolA*)	*tolB*, *pal*, *cpoB*			+
4	LP50	Δ(*tolA-pal*)	*tolQR*, *cpoB*			−
5	BL78	Δ*cpoB*	*tolQRAB*, *pal*			−
6	LP57	Δ(*tolQ-cpoB*)				−
7	LP57	Δ(*tolQ-cpoB*)		pBAD33	P_{BAD}::	−
8	LP57	Δ(*tolQ-cpoB*)		pMG45	P_{BAD}::*tolB*	−
9	LP57	Δ(*tolQ-cpoB*)		pCH546	P_{BAD}::*cpoB*	−
10	LP57	Δ(*tolQ-cpoB*)		pCH518	P_{BAD}::*tolB pal*	−
11	LP57	Δ(*tolQ-cpoB*)		pCH545	P_{BAD}::*pal cpoB*	−
12	LP57	Δ(*tolQ-cpoB*)		pCH528	P_{BAD}::*tolB pal cpoB*	+
13	LP57	Δ(*tolQ-cpoB*)		pCH544	P_{BAD}::*tolB pal*^{0} *cpoB*	−
14	LP57	Δ(*tolQ-cpoB*)		pCH548	P_{BAD}::*tolB pal cpoB*^{0}	−
15	LP49	Δ*tolA*	*tolQRB*, *pal*, *cpoB*			−
16	LP57	Δ(*tolQ-cpoB*)		pCH528	P_{BAD}::*tolB pal cpoB*	−

[a]Strains lysogenic for λCH536 (P_{lac}::*gfp-malF*$^{2-39}$-*rodZ*$^{139-255}$-*tolA*$^{294-421}$) (rows 1 to 14) or λCH543 (P_{lac}::*gfp-malF*$^{2-39}$-*rodZ*$^{139-255}$) (rows 15 and 16) and transformed with the indicated plasmid (rows 7 to 14 and 16) were grown for ~3.5 mass doublings to OD_{600} = 0.5 to 0.6 in M9-maltose medium with 37 μM IPTG and either no (all rows) or 0.01% (rows 7 to 14 and 16) arabinose. Note that the results in rows 7 to 14, and 16 were the same with or without the addition of arabinose. See also Table S2.
[b]GFP fluorescence distributed evenly along the periphery of cells (−) or accumulated at sites of cell constriction (+).
[c]Genes of the *tolQ-cpoB* cluster that are still present on the chromosome.

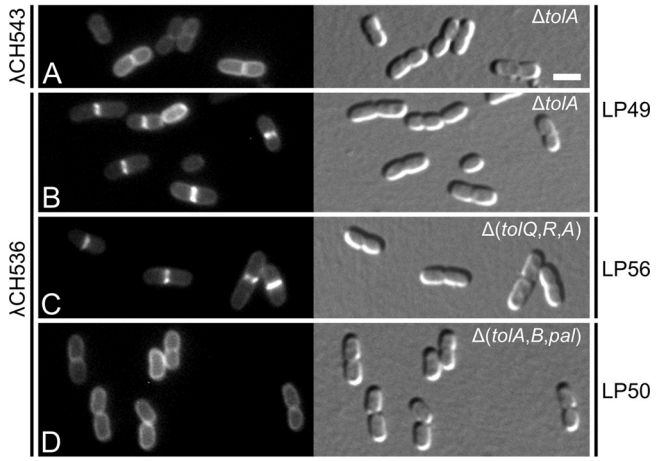

FIG 4 Recruitment of TolAIII (TolA$^{294-421}$) to division sites does not require TolQ or TolR. Fluorescence (left) and DIC (right) images of lysogenic derivatives of strains LP49 (Δ*tolA*) (A and B), LP56 (Δ[*tolQ-tolA*]) (C), and LP50 (Δ[*tolA-pal*]) (D), carrying λCH543 (P_{lac}::*gfp-malF*$^{2-39}$-*rodZ*$^{139-255}$) (A), or λCH536 (P_{lac}::*gfp-malF*$^{2-39}$-*rodZ*$^{139-255}$-*tolA*$^{294-421}$) (B to D) integrated in the chromosome. Cells were grown for ~3.5 mass doublings to OD_{600} = 0.5 to 0.6 in M9-maltose medium with 37 μM IPTG and imaged live. Bar equals 2 μm.

accumulated at the vast majority (~90%) of division sites in LP57(λCH536) cells carrying plasmid pCH528 (P_{BAD}::*tolB pal cpoB*), even in the absence of added arabinose (Fig. 5B, Table 3, and Table S2). Notably, such accumulation at division sites did not occur when, instead of plasmid pCH528, cells carried derivatives that lacked intact *tolB* (pCH545 [P_{BAD}::*pal cpoB*]), *pal* (pCH544 [P_{BAD}::*tolB pal*^{0} *cpoB*]) or *cpoB* (pCH518 [P_{BAD}::*tolB pal*]), even in the presence of arabinose (Fig. 5C to E, Table 3, and Table S2). Rather, GFP-M-L-TolAIII appeared dispersed along the membrane in almost all (>95%) cells lacking TolB or CpoB as well as in the great majority (>87%) of those lacking intact Pal.

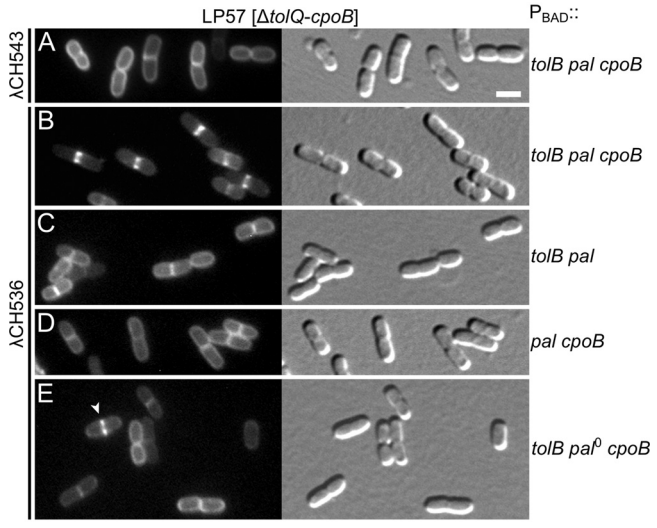

FIG 5 Efficient recruitment of TolAIII (TolA$^{294-421}$) to division sites requires TolB, Pal, and CpoB. Fluorescence (left) and DIC (right) images of strain LP57 (Δ[*tolQ-cpoB*]) carrying λCH543 (P_{lac}::*gfp-malF*$^{2-39}$-*rodZ*$^{139-255}$) (A), or λCH536 (P_{lac}::*gfp-malF*$^{2-39}$-*rodZ*$^{139-255}$-*tolA*$^{294-421}$) (B to E) integrated in the chromosome, and harboring plasmid pCH528 (P_{BAD}::*tolB pal cpoB)* (A and B), pCH518 (P_{BAD}::*tolB pal*) (C), pCH545 (P_{BAD}::*pal cpoB*) (D), or pCH544 (P_{BAD}::*tolB pal*^{0} *cpoB)* (E). Cells were grown for ~3.5 mass doublings to OD_{600} = 0.5 to 0.6 in M9-maltose medium with 37 μM IPTG and imaged live. Bar equals 2 μm. Plasmid pCH544 is identical to pCH528, except for a frameshift at codon 53 of the Pal open reading frame (ORF). The arrowhead in panel E points at a rare septal accumulation of the GFP-M-L-TolAIII fusion that was seen in this population of cells at an approximately 6-fold lower frequency than that of panel B (see Table S2).

Some of these cells did still show an apparent accumulation of GFP-M-L-TolAIII at the site of constriction (e.g., Fig. 5E, arrowhead), but their frequency was at least 6-fold lower than in populations of LP57(λCH536)/pCH528 cells producing all three proteins (Fig. 5; Table S2).

We infer that all three of the TolB, Pal, and CpoB proteins are required for the efficient recruitment of the GFP-M-L-TolAIII fusion to sites of cell constriction.

Septal recruitment of TolQ in the absence of FtsN. FtsN is the last core protein to accumulate strongly at the SR and helps trigger the active cell constriction phase of the division process (1, 2, 7, 8). We previously showed that TolQ and TolA fail to accumulate at SRs in filaments of the FtsN-depletion strain CH34/pMG20 (Δ*ftsN*/P_{BAD}::^{TT}*bfp-ftsN*$^{71-105}$), implying a direct or indirect role for FtsN in SR recruitment of the Tol proteins (23). An indirect role seemed most likely because production of the Tat-targeted periplasmic fusion containing the small essential domain of FtsN (^{TT}BFP-FtsN$^{71-105}$) was sufficient to restore both cell division and the recruitment of TolQ and TolA to constriction sites of these Δ*ftsN* cells (23), and because a green fluorescent version of this periplasmic fusion (^{TT}GFP-FtsN$^{71-105}$) did not accumulate at these sites but appeared evenly distributed throughout the periplasm (7).

An indirect role for FtsN in septal recruitment was shown to be correct for the full-length TolA protein because GFP-TolA still accumulated at division sites in Δ*ftsN* *ftsA*^{E124A} cells, which lack any part of the FtsN protein and rely on a mutant superfission variant of the FtsA protein for viability instead (13). However, TolQ was not included in this study, and two-hybrid analyses have since provided evidence for a direct interaction between periplasmic portions of TolQ and FtsN, suggesting that septal recruitment of TolQ might involve direct physical contact with FtsN (38).

To assess whether TolQ can still recognize division sites in the complete absence of FtsN, we examined the localization of plasmid-encoded TolQ-GFP in cells of strain CH238 (Δ[*tolQ-cpoB*] *ftsB*^{E56A}) and of its Δ*ftsN* derivative CH239 (Δ[*tolQ-cpoB*] *ftsB*^{E56A} Δ*ftsN*). Besides lacking the *tolQ-cpoB* gene cluster, these strains also carry a strong superfission allele of the *ftsB* division gene, which promotes cell constriction and allows cells to survive and divide in the complete absence of FtsN (8). The strains displayed phenotypes typical for *ftsB*^{E56A} *ftsN*$^{+}$ (CH238) or *ftsB*^{E56A} Δ*ftsN* (CH239) cells (8). Thus, CH238 cells were smaller than normal and displayed some cell shape defects (Fig. 6A, C, and F) while CH239 cells were modestly elongated (Fig. 6B, D, and G).

Notably, TolQ-GFP still accumulated strongly at constriction sites in cells of both strains (Fig. 6A and B), demonstrating that the reported interaction between FtsN and TolQ (38) is not required for recruitment of TolQ to these sites. We conclude that FtsN plays an indirect role in the recruitment of TolQ to division sites.

Role of FtsN in septal recruitment of TolAII. We also examined the localization of GFP-TolA in CH239 (Δ[*tolQ-cpoB*] *ftsB*^{E56A} Δ*ftsN*) cells. Surprisingly, this fusion failed to accumulate at sites of cell constriction. Instead, GFP-TolA distributed along the cell periphery and actually appeared to be excluded to some extent from constriction sites in a subset of cells (Fig. 6D; Fig. 7A). The GFP-M-TolAII fusion (GFP-MalF$^{2-39}$-TolA$^{47-292}$) showed a similar distribution in this strain (Fig. 6G; Fig. 7D), which was consistent with the evidence discussed above where domain II determined the localization pattern of the TolA protein in the absence of other Tol-Pal proteins and CpoB. In contrast, both GFP-TolA and GFP-M-TolAII still accumulated at constriction sites in strain CH238 (Δ[*tolQ-cpoB*] *ftsB*^{E56A}), indicating that their failure to do so in CH239 (Δ[*tolQ-cpoB*] *ftsB*^{E56A} Δ*ftsN*) cells was due to the absence of *ftsN* rather than to the presence of the *ftsB*^{E56A} allele (Fig. 6C and F). Indeed, septal accumulation of either fusion in CH239 cells could be restored by production of the periplasmic fusion containing the essential peptide of FtsN (^{E}FtsN), encoded on plasmid pMG20 (P_{BAD}::^{TT}*bfp-ftsN*$^{71-105}$) (Fig. 6E and H). Western blot analyses indicated that the absence of FtsN did not reduce the stability of GFP-TolA or GFP-M-TolAII (Fig. S5). Together, these results implied that the ability of TolA, and more specifically of its TolAII domain, to accumulate at constriction sites in the absence of the other Tol-Pal proteins and CpoB is dependent on some function

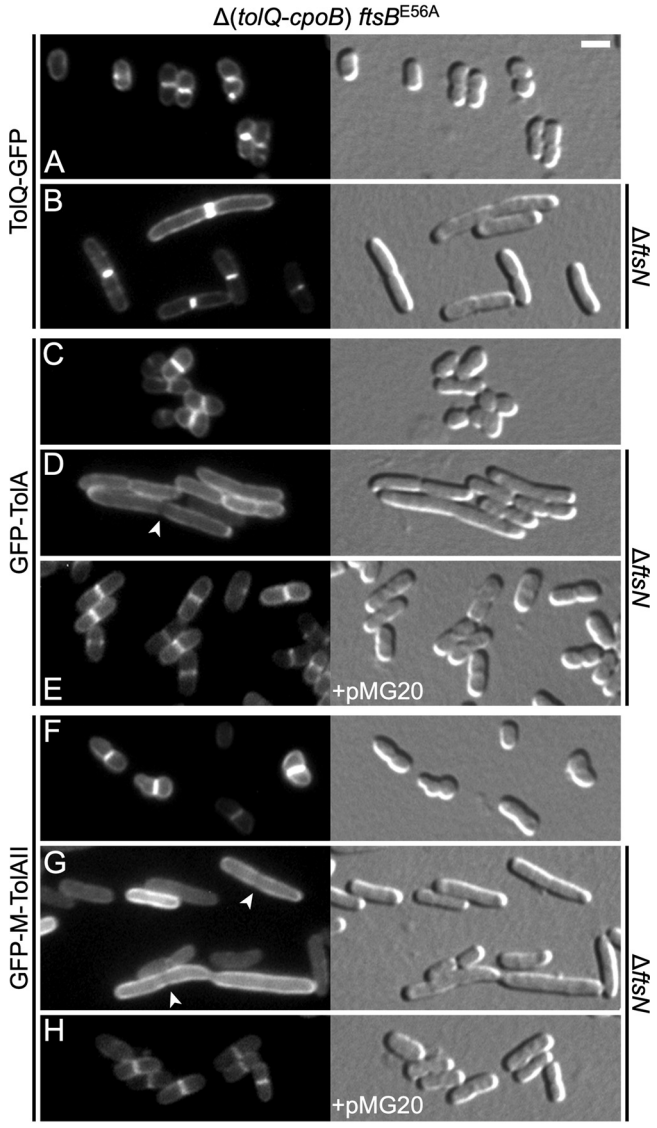

FIG 6 Localization of TolQ and TolA in the absence of FtsN and other Tol-Pal proteins. GFP fluorescence (left) and DIC (right) images of CH238 (Δ[*tolQ-cpoB*] *ftsB*^{E56A}) (A, C, and F) or CH239 (Δ[*tolQ-cpoB*] *ftsB*^{E56A} Δ*ftsN*] (all other panels) cells carrying either plasmid pCH516 (P_{lac}::*tolQ-gfp*) (A, B), or lysogenic for λNP4 (P_{lac}::*gfp-tolA*) (C to E) or λCH549 (P_{lac}::*gfp-malF*$^{2-39}$ *-tolA*$^{47-292}$) (F to H). The cells in panels E and H additionally carried plasmid pMG20 (P_{BAD}::^{TT}*bfp-ftsN*$^{71-105}$), encoding a periplasmic fusion containing the essential domain of FtsN (^{E}FtsN). Cells were grown for ~3.5 mass doublings to OD_{600} = 0.5 to 0.6 in M9-maltose medium with 5 μM (A and B) or 37 μM (C to H) IPTG and with 0.1% (E and H) or no (all others) arabinose, and imaged live. Bar equals 2 μm. Note that both full-length TolA (D) and the TolAII domain (G) fail to accumulate at division sites in the complete absence of FtsN and actually appear to be partially excluded from such sites in some of the cells (arrowheads).

of ^{E}FtsN that is not readily compensated for by FtsB^{E56A} when FtsN is completely absent.

The likely reason that GFP-TolA was previously observed to still accumulate at constriction sites in Δ*ftsN ftsA*^{E124A} cells is that these also still produced all five Tol-Pal proteins and CpoB (13). Based on our results described above, this would have allowed recruitment of full-length TolA to division sites by TolQ (in a TolAI-dependent manner) and possibly also by TolB, Pal, and CpoB (in a TolAIII-dependent manner), even in the absence of FtsN. Accordingly, septal accumulation of GFP-TolA (Fig. 7B and C) but not that of GFP-M-TolAII (Fig. 7E and F) could be restored in CH239 (Δ[*tolQ-cpoB*] *ftsB*^{E56A}

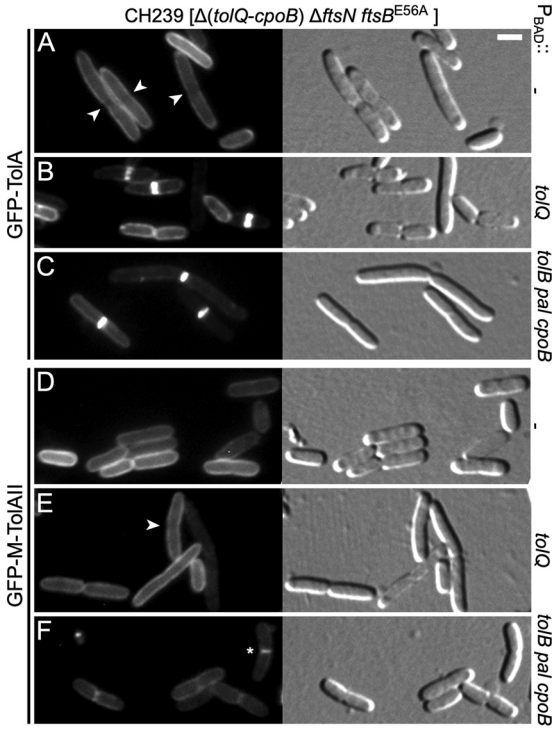

FIG 7 Localization of TolA in the absence of FtsN depends on other Tol-Pal proteins and CpoB. Fluorescence (left) and DIC (right) images of live CH239 (Δ[*tolQ-cpoB*] *ftsB*^{E56A} Δ*ftsN*) cells lysogenic for λNP4 (P_{lac}::*gfp-tolA*) (A to C) or λCH549 (P_{lac}::*gfp-malF*$^{2-39}$ -*tolA*$^{47-292}$) (D to F), and carrying plasmid pBAD33 (P_{BAD}::) (A, D), pLP146 (P_{BAD}::*tolQ*) (B, E), or pCH528 (P_{BAD}::*tolB pal cpoB)* (C, F). Cells were grown for ~3.5 mass doublings to OD_{600} = 0.5 to 0.6 in M9-maltose medium with 37 μM IPTG. Arabinose was either omitted (C, F) or was added to 0.02% when cultures reached OD_{600}= 0.3 (all others). Bar equals 2 μm. Arrowheads point at division sites at which GFP-TolA (A) or GFP-M-TolAII (E) fluorescence appears relatively low. The star in panel F marks a cell in which GFP-M-TolAII appears to have weakly accumulated at the site of constriction.

Δ*ftsN*) cells upon production of TolQ from plasmid pLP146 (P_{BAD}::*tolQ*) or upon coproduction of the TolB, Pal, and CpoB proteins from pCH528 (P_{BAD}::*tolB pal cpoB*).

FtsN is proposed to indirectly stimulate the activities of sPG synthases FtsW/PBP3 (FtsW/FtsI, FtsWI) and PBP1B via interactions with FtsA in the cytoplasm and with the FtsBLQ subcomplex in the periplasm, while superfission variants of FtsA (such as FtsA^{E124A}) or FtsBLQ (such as FtsB^{E56A}LQ) are thought to spontaneously adopt conformations that promote sPG synthase activities even when FtsN is lacking (2, 6, 8, 9, 12, 18). In addition, FtsN was found to interact directly with PBP1B and to modestly stimulate its PG synthase activities *in vitro* (16, 18, 21, 92). Thus, the fact that neither TolQ nor TolA accumulated at SRs in FtsN-depleted, but otherwise wild-type, cells suggested that their recruitment may, at least in part, depend on sPG synthesis (23). As shown above, neither PBP1A nor PBP1B is required for recruitment of TolQ-GFP or GFP-TolA to constriction sites and, as might be expected, the same was true for recruitment of the GFP-M-TolAII fusion (Fig. S2).

To assess whether sPG synthesis by the essential sPG synthase FtsWI is required for recruitment of TolQ and/or TolA to constriction sites, we monitored TolQ-GFP or GFP-TolA localization after blocking the transpeptidase activity of FtsWI with aztreonam (93, 94). For these experiments, we employed strains that also produced a newly developed functional fluorescent version of the ZipA protein, as described in the following section.

Functional fluorescent versions of the essential division protein ZipA. ZipA is a type Ib (N-out) bitopic inner membrane protein and an essential component of the SR (91). It directly binds FtsZ and FtsA, helps anchor FtsZ polymers to the IM and accumulates with FtsZ and FtsA at the prospective division site during the earliest stages of SR development (91, 95–98). ZipA contains 328 residues that form a small periplasmic peptide (ZipA$^{1-3}$), a TM

TABLE 4 Functional fluorescent ZipA sandwich fusions

		Result in LB[b]			Result in M9-glucose medium[c]		
Strain[a]	Genotype	Length[d]	Width[d]	*n*[e]	Length[d]	Width[d]	*n*[e]
TB28	wt	4.18 (0.88)	0.90 (0.07)	838	2.43 (0.50)	0.96 (0.08)	2,027
CH119	TB28, *yfeN<>aph*	4.24 (0.89)	0.90 (0.07)	609	2.53 (0.53)	0.97 (0.09)	1,764
CH125	CH119, *zipA-rfp*^{SW}	4.14 (1.00)	0.87 (0.09)	1622	2.74 (0.58)	0.97 (0.08)	2,177
CH128	CH119, *zipA-*$_{SF}$*gfp*^{SW}	4.18 (0.97)	0.96 (0.08)	1480	2.61 (0.57)	0.98 (0.09)	2,158

[a]Cells were chemically fixed, imaged with phase contrast optics, and analyzed using MicrobeJ software (115).
[b]Cells were grown for ~5 mass doublings to OD_{600} = 0.65 to 0.70 before fixation.
[c]Cells were grown for ~3.5 mass doublings to OD_{600} = 0.55 to 0.60 before fixation.
[d]Mean in micrometers, with standard deviation in parentheses.
[e]Number of cells measured.

helix (ZipA$^{4-27}$), a highly charged domain (ZipA$^{29-85}$), a flexible linker domain that is rich in proline and glutamine residues (P/Q domain, ZipA$^{86-185}$), and a globular FtsZ-binding domain (ZipA$^{186-328}$) (Fig. S6) (91, 95, 99). In our experience, the production of ZipA variants with N-terminal extensions is poorly tolerated by cells, and, although fusions of fluorescent proteins to the C terminus of ZipA still bind FtsZ and localize to the SR, they cannot compensate for the absence of native ZipA (91, 100; and data not shown). Because a functional fluorescent version of ZipA would be useful for a variety of studies, we explored whether the in-frame insertion of a fluorescent protein (FP) within the P/Q linker domain of ZipA would yield a ZipA'-FP-'ZipA sandwich fusion (ZipA-FP^{SW}, for short) that retains ZipA function. We and others previously used a similar approach to obtain functional fluorescent versions of MreB and FtsZ (90, 101).

To replace chromosomal *zipA* with alleles encoding ZipA-FP^{SW} fusion proteins, we built recombineering strains that allow the use of *galK* as a (counter)selectable marker (102). For example, strain CH121/pCH279 (Δ*galK* [λc1857 *cro-bioA<>tetA*] *zipA<>*P$_{EM7}$::*galK yfeN<>aph*/P$_{lac}$::*ftsA*^{R286W}) does not carry *galK* at its normal chromosomal position (Δ*galK*) but rather carries it on an expression cassette (P$_{EM7}$::*galK*) that replaced codons 161 to 164 of *zipA*, which encode poorly conserved residues within the P/Q domain of ZipA (Fig. S6). Despite lacking intact ZipA, these cells grow well in the presence of IPTG (isopropyl-β-D-thiogalactopyranoside) due to the production of the superfission variant of FtsA (R286W) (103), encoded on plasmid pCH279. The P$_{EM7}$::*galK* cassette in these cells was next replaced via recombineering with mCherry (red fluorescent protein [RFP]) or superfolder GFP ($_{SF}$GFP) open reading frames using 2-deoxy-galactose to counterselect GalK$^+$ nonrecombinants. The recombinants grew well in the absence of IPTG in both cases, suggesting they were phenotypically ZipA$^+$, and the recombinant *zipA-rfp*^{SW} or *zipA-*$_{SF}$*gfp*^{SW} alleles could subsequently be readily introduced into TB28 (wt) cells by P1-mediated cotransduction with the nearby *yfeN<>aph* marker. Thus, the substitution of four residues within the P/Q domain of ZipA with RFP indeed yielded a functional red fluorescent ZipA$^{1-160}$-RFP-ZipA$^{165-328}$ sandwich fusion (ZipA-RFP^{SW}), and substitution with $_{SF}$GFP similarly yielded a functional green fluorescent version (ZipA-$_{SF}$GFP^{SW}).

Notably, the dimensions of CH125 (*zipA-rfp*^{SW} Δ*yfeN*) and CH128 (*zipA-*$_{SF}$*gfp*^{SW} Δ*yfeN*) cells were virtually identical to those of the *zipA*$^+$ parents CH119 (Δ*yfeN*) and TB28 (wt) upon growth in either rich or minimal medium (Table 4), indicating that the sandwich fusions support normal cell division. In addition, fluorescence microscopy showed that both fusions localize to the SR, as expected (Fig. 8 and 9 and data not shown). Thus, fluorescent versions of ZipA that retain most, if not all, of the functionality of the native protein are available.

Septal recruitment of TolQ and TolA depends on FtsI (PBP3) PG transpeptidase activity. Accumulation of ZipA is a good proxy for the presence of a Z-ring and its localization should not be affected by inhibition of sPG synthesis (7, 96, 104). To assess the effects of aztreonam on the localization of TolQ-GFP and GFP-TolA, therefore, we used cells in which the localization of ZipA could be monitored as well. Strain CH241/pCH633 (Δ*tolQ zipA-rfp*^{SW}/P$_{BAD}$::*tolQ-gfp*) is a Δ*tolQ* derivative of CH125 (see above) that encodes ZipA-RFP^{SW} under native regulatory control on the chromosome and TolQ-

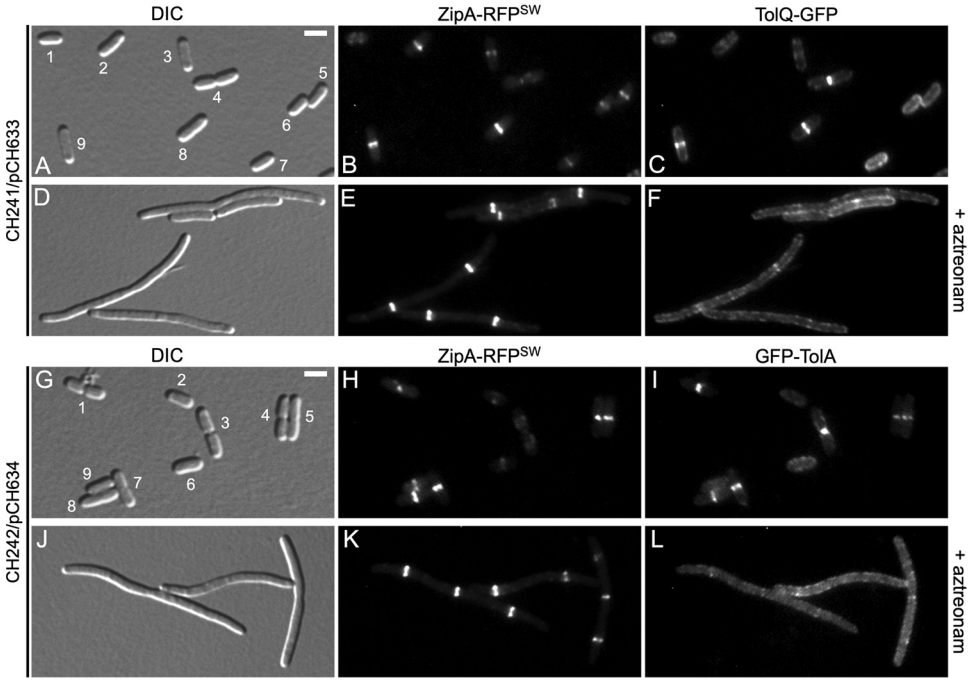

FIG 8 Septal accumulation of TolQ and TolA depends on FtsI (PBP3) activity. Live cells were imaged with DIC (A, D, G, and J), RFP-fluorescence (B, E, H, and K), and GFP fluorescence (C, F, I, and L) optics. Two cultures of each strain were grown in parallel for ~3.5 mass doublings to OD_{600} = 0.5 to 0.6 in M9-maltose medium without arabinose (A to F) or in M9-glucose medium with 0.02% arabinose (G to L). Aztreonam (to 1 μg/mL) was added to one of the parallel cultures (D to F and J to L) ~2 mass doublings before imaging. Bar equals 2.0 μm (A to C and G to I) or 2.5 μm (D to F and J to L). (A to F) Cells of strain CH241/pCH633 (Δ*tolQ zipA-rfp*^{SW}/P_{BAD}::*tolQ-gfp*). Note the presence in panels A to C of small cells without a ZipA-RFP^{SW} (~ZipA) or TolQ-GFP (~TolQ) ring (cell 1), or with a ZipA ring and peripheral distribution of TolQ (cells 5, 6, and 7); larger cells with a ZipA ring in which TolQ has not yet accumulated in a clear ring (cells 2 and 3); constricting cells with both a ZipA ring and a TolQ ring (cells 8 and 9); and a cell with TolQ strongly accumulated at the deep constriction from which ZipA has mostly departed already (cell 4). In comparison, note the failure of TolQ to strongly accumulate with ZipA rings in the aztreonam-treated cells in panels D to F. (G to L) Cells of strain CH242/pCH634 (Δ*tolA zipA-rfp*^{SW}/P_{BAD}::*gfp-tolA*). Note the presence in panels G to I of smaller nonconstricting cells with a ZipA ring and a peripheral distribution of GFP-TolA (~TolA) (cells 2, 6, and 9); constricting cells with both a ZipA ring and a TolA ring (cells 4, 5, 7, and 8); and cells with a deep constriction from which ZipA has mostly already relocated but at which TolA is still strongly concentrated (cells 1 and 3). In comparison, note the failure of TolA to strongly accumulate with ZipA rings in the aztreonam-treated cells in panels J to L.

GFP under control of the *ara* regulatory region on the plasmid. Upon growth of CH241/pCH633 in medium without aztreonam, a clear ZipA-RFP^{SW} ring was observed in most preconstriction and constricting cells (Fig. 8A and B). In contrast, TolQ-GFP localized in a somewhat grainy pattern along with the entire envelope of preconstriction cells and appeared to strongly accumulate with ZipA-RFP^{SW} only in cells with a visible constriction (Fig. 8A to C). In addition, in deeply constricted cells that were likely about to separate into two sisters, TolQ-GFP still accumulated at the cell junction while most ZipA-RFP^{SW} molecules had already departed this site (e.g., cell 4 in Fig. 8A to C). These results are consistent with previous evidence showing that the Tol-Pal proteins join the SR machinery in an FtsN-dependent manner at a relatively late stage of the division cycle that is near coincident with the initiation of active cell fission (23), and that a ZipA-mCherry fusion departs this machinery relatively early during the terminal stages of the fission process (105).

As expected, growth of CH241/pCH633 in the presence of aztreonam (1 μg/mL) led to the formation of filamentous cells with ZipA-RFP^{SW} strongly accumulated in one medial ring or multiple evenly spaced rings. In contrast, the bulk of TolQ-GFP fluorescence formed a grainy pattern along the cell periphery, and the fusion accumulated with any resident ZipA-RFP^{SW} ring only weakly, if at all (Fig. 8D to F).

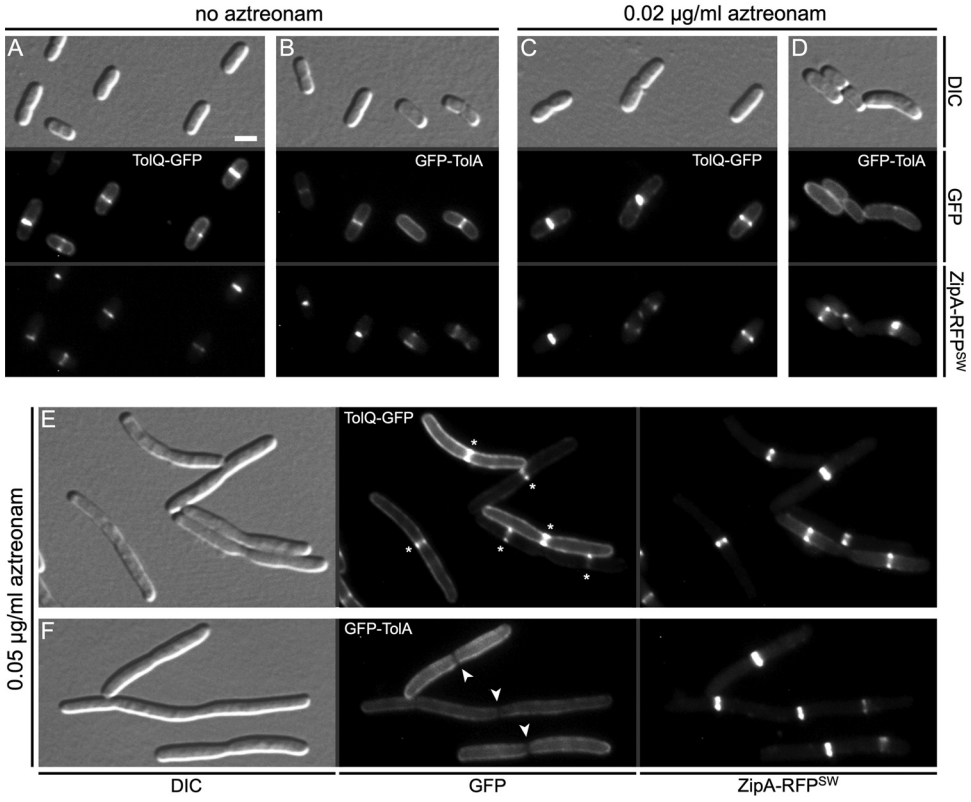

FIG 9 Septal accumulation of TolA is very sensitive to interference with PBP3 activity. Live cells were imaged with DIC, and GFP and RFP fluorescence optics as indicated. Cultures of strain CH244 (Δ[*tolQ-cpoB*) *zipA-rfp*^{SW}) carrying pCH633 (P_{BAD}::*tolQ-gfp*) (A, C, and E) or pCH634 (P_{BAD}::*gfp-tolA*) (B, D, and F) were grown in parallel for ~3.5 mass doublings to OD_{600} = 0.6 to 0.7 in M9-glucose medium with 0.005% (A, C, and E) or 0.03% (B, D, and F) arabinose. Aztreonam was omitted (A and B) or added to 20 ng/mL (C and D) or 50 ng/mL (E and F) ~2 mass doublings before imaging. Bar equals 2.0 μm. Sites of cell constriction with strong accumulations of ZipA-RFP^{SW} are evident in panels E and F. While clear accumulations of TolQ-GFP at these sites can still be seen (E, stars), GFP-TolA appears to be partially excluded from such sites (F, arrowheads).

Strain CH242/pCH634 (Δ*tolA zipA-rfp*^{SW}/P_{BAD}::*gfp-tolA*) was similarly used to monitor the effects of aztreonam on the localization pattern of TolA. As illustrated in Fig. 8, the localization patterns of GFP-TolA in untreated (Fig. 8G to I) and aztreonam-treated (Fig. 8J to L) CH242/pCH634 cells were very similar to those of TolQ-GFP in untreated (Fig. 8A to C) and treated (Fig. 8D to F) CH241/pCH633 cells, respectively.

Hence, recruitment of both the TolQ and TolA protein to the SR largely depends on the TP activity of PBP3 (FtsI). These results are consistent with the evidence that septal recruitment of both TolQ (Fig. 6B) and TolA (13) depends on FtsN in an indirect manner and suggest that active sPG synthesis by FtsWI plays an important role in attracting both these proteins to the site of constriction.

Septal recruitment of GFP-TolA in the absence of other Tol proteins and CpoB is particularly sensitive to interference with FtsI (PBP3) activity. Although the *ftsB*^{E56A} superfission allele allows cells to grow and divide in the absence of FtsN, *ftsB*^{E56A} Δ*ftsN* cells display a mild filamentous/chaining phenotype, suggesting that sPG synthesis is inefficient or slow (8, 15). Therefore, the failure of GFP-TolA and GFP-TolAII to accumulate at constriction sites of CH239 (Δ[*tolQ-cpoB*] *ftsB*^{E56A} Δ*ftsN*) cells (Fig. 6 and 7) suggested the possibility that the ability of TolA to concentrate at these sites in the absence of other Tol-Pal components and CpoB is particularly sensitive to the activity level of FtsWI sPG synthases.

To further explore this possibility, we examined the effects of low concentrations of aztreonam on the location of TolQ-GFP or GFP-TolA in cells of strain CH244 (Δ[*tolQ-cpoB*] *zipA-rfp*^{SW}) harboring pCH633 (P_{BAD}::*tolQ-gfp*) or pCH634 (P_{BAD}::*gfp-tolA*), respectively. Cells

of this strain lack the Tol-Pal proteins and CpoB but produce native FtsB and FtsN, and ZipA-RFP^{SW} as the sole source of ZipA. In the absence of aztreonam, TolQ-GFP and GFP-TolA accumulated at the vast majority (>90%) of constriction sites in CH244 cells, as expected (Fig. 9A and B; Table S3). Exposure to 20 ng/mL aztreonam for 3.5 h caused only a slight elongation of cells and did not noticeably affect TolQ-GFP or ZipA-RFP^{SW} localization (Fig. 9C and D). However, this low drug concentration significantly affected the localization pattern of GFP-TolA. Thus, the fusion now accumulated at only a minority (<30%) of constriction sites and instead appeared dispersed along the periphery of most cells (Fig. 9D; Table S3). Upon exposure to 50 ng/mL aztreonam, the cells became more distinctly elongated but most (~90%) still showed at least one clear constriction (Fig. 9E and F). While a significant fraction of TolQ-GFP molecules still accumulated at these sites (Fig. 9E; Table S3), this was not observed with GFP-TolA. In fact, the fusion often appeared partially excluded from sites of constriction (Fig. 9F; Table S3), reminiscent of its localization pattern in CH239 (Δ[*tolQ-cpoB*] *ftsB*^{E56A} Δ*ftsN*) cells in the absence of aztreonam (Fig. 6D and 7A). These results support the idea that septal accumulation of TolA in the absence of other Tol-Pal proteins and CpoB is indeed significantly more sensitive to the activity level of FtsWI than septal accumulation of TolQ under the same conditions.

DISCUSSION

We generated an isogenic set of *E. coli* TB28 (MG1655, Δ*lacIZYA*) (106) derivatives in which one or more of the genes that encode the five proteins of the Tol-Pal system and CpoB were substituted with *aph* (Kan^r). All strains lacking one or more components of the Tol-Pal system showed a similar cell chaining phenotype in low-osmotic medium, and complementation experiments indicated that this phenotype was not due to polar effects of the substitutions on the expression of nearby genes (Fig. 1, and data not shown). Although not detailed here, we note that the newly generated Tol-Pal$^-$ strains also shared other morphological features with the previously characterized strains FB20229 (*tolA::EZTNKAN-2*), MG5 (Δ*pal*), *and* MG4 (Δ[*tolQ-pal*]) that are evident even when cell chaining is substantially suppressed by growth in a medium of standard osmolarity (LB or M9). These include a high fraction of cells with a visible constriction, a local expansion of the periplasmic space at sites of cell constriction, a prodigious release of large OM vesicles from constriction sites and cell poles, and a squat cell shape ([23] and data not shown). The results are consistent with previous work on subsets of *tol* or *pal* mutants of *E. coli* (23, 37, 38, 40, 41) and other Gram-negative species (24, 80–84), and imply that the lack of each one of the five Tol-Pal proteins causes a delay in OM invagination during cell fission.

In contrast, lack of the CpoB protein did not lead to an overt cell division phenotype (Fig. 1L), suggesting it plays a relatively minor or redundant role in the process. The lack of CpoB also did not prevent TolQ-GFP or GFP-TolA from accumulating at constriction sites (Fig. 2; Table 1), implying that neither the other Tol-Pal proteins nor CpoB is required for full-length TolQ or TolA to recognize these sites.

Our studies of domain deletion/substitution derivatives of GFP-TolA showed that periplasmic domain II of TolA (TolA$^{47-292}$) is responsible for the recognition of constriction sites in cells lacking all other Tol-Pal proteins and CpoB (Fig. 2; see Fig. S2 in the supplemental material; Table 1). Other than linking IM-bound domain TolAI with periplasmic domain TolAIII, the precise properties and functions of TolAII are still enigmatic. It consists of 263 residues with Ala (40%), Lys (19%), Glu (15%), and Asp (5%) as the most abundant and contains several tandem repeat sequences. Circular dichroism, analytical centrifugation, solution X-ray scattering, and molecular modeling data indicate that TolAII has an elongated stalk-like shape that is likely formed by a coiled-coil of three extended α-helices with one running anti-parallel to the other two (48, 52, 53). This arrangement is thought to allow for structural plasticity of TolAII, which may be critical in coupling the dissipation of PMF by TolAI-bound TolQR complexes in the IM to movement of the TolAIII domain toward Pal or Pal-TolB complexes in the OM (42, 43, 46, 53, 58).

How TolAII or TolQ recognize constriction sites is unclear. The failure of Tol-Pal proteins to accumulate at septal rings in FtsN-depleted filaments suggested that their recruitment might depend on active cell constriction and the accompanying synthesis of sPG (23). Accordingly, whereas the PG synthases PBP1A and PBP1B were individually dispensable for their septal localization (Fig. S2), TolQ and TolA failed to accumulate at constrictions and/or septal rings upon inhibition of the transpeptidase activity of the FtsWI sPG synthase with aztreonam (Fig. 8). Still, interesting differences in the localization behavior of TolQ and TolA in the absence of other Tol-Pal proteins and CpoB were noted. First, septal localization of TolA (and TolAII) appeared significantly more dependent on normal FtsWI activity than that of TolQ. This was seen when Δ(*tolQ-cpoB*) cells were treated with low concentrations of aztreonam (Fig. 9; Table S3) and in Δ(*tolQ-cpoB*) Δ*ftsN ftsB*^{E56A} cells in which FtsWI activity is presumed suboptimal due to the absence of FtsN (Fig. 6). Under these conditions, moreover, GFP-TolA or GFP-M-TolAII fusions appeared partially depleted from some constriction sites, an unexpected pattern that we have not observed with TolQ-GFP thus far (Fig. 6, 7, and 9; Table S3). Together with the fact that TolAII (periplasm) and TolQ (mostly IM and cytoplasm) predominantly reside in different cell compartments (47, 107, 108), these results render it unlikely that TolAII and TolQ recognize the same septal target. The observation that GFP-TolA or GFP-M-TolAII fusions can become partially depleted from constriction sites in Δ(*tolQ-cpoB*) cells with suboptimal sPG synthase activity suggests that the TolAII domain also interacts relatively weakly with nonseptal molecules that are distributed along the cell envelope of the cylindrical part(s) of the cell. The latter may then hinder free diffusion of TolA into the septal region when the concentration of the septal target is suppressed. In any event, although it is now clear that septal recruitment of both TolQ and TolA requires the catalytic activities of FtsWI, additional work will be required to identify the actual direct septal targets of TolQ and TolAII.

Studies of domain deletion/substitution derivatives of GFP-TolA further revealed that septal accumulation of TolA can also be mediated by TolAI or TolAIII provided that one or more of the other products of the *tol-cpoB* gene cluster is present in the cell as well. The presence of TolQ was sufficient to recruit GFP-TolAI fusion proteins to cell constrictions. In contrast, recruitment of GFP-M-L-TolAIII to such sites was not dependent on TolQ or TolR but required the coproduction of TolB, Pal, and CpoB.

Genetic and chemical cross-linking experiments provided evidence that TolAI interacts directly with TolQ within the IM bilayer, involving contacts between the TM of TolA and TM1 of TolQ (49, 50). Our results indicate that this interaction is sufficiently strong for TolQ to recruit TolA to cell constrictions and that TolR, TolB, Pal, and CpoB are dispensable for this interaction to occur (Fig. 3 and 7, and S4).

In contrast, the more elaborate requirements for septal recruitment of TolA$^{294\text{-}421}$ (~TolAIII) suggest it involves multiple interactions. TolB and CpoB were previously found to bind TolA$^{294\text{-}421}$ directly and noncompetitively, although relatively weakly as well (K_d in 40 to 60 μM range) (57, 58, 76). Based on chemical cross-linking results, TolAIII was also thought to directly engage Pal (42, 64). However, supporting genetic or biochemical evidence for a direct TolA-Pal interaction has been lacking, and subsequent evidence for TolB acting as an intermediary *in vitro* suggests that TolA-TolB and TolB-Pal heterodimers and TolA-TolB-Pal heterotrimers are the more physiologically relevant protein complexes existing *in vivo* (58, 69). Because TolB, Pal, and CpoB are all required for the efficient septal accumulation of GFP-M-L-TolAIII, it is possible that this is driven by the formation of four-member complexes (~CpoB-TolAIII-TolB-Pal) at cell constriction sites. The tripartite TolAIII-TolB-Pal complex is predicted to be quite unstable (58), but it is conceivable that the addition of CpoB has a stabilizing effect. In this regard, it is interesting that recent residue coevolution and molecular docking studies support the existence of an even larger TolB-centric complex with TolB bound to TolR, TolA, Pal, and CpoB (109). However, one confounding issue is understanding why any proposed multimember complex containing TolAIII, TolB, Pal, and CpoB would preferentially exist at the constriction site of cells that cannot form functional TolQRA

complexes in the inner membrane (such as those shown in Fig. 4B and C, 5B, and 7C). Septal recruitment of both TolB and Pal is dependent on the presence of functional TolQ, R, and A but independent of CpoB (40) (our unpublished results). Thus, it is not obvious how they help drive GFP-M-L-TolAIII to septal sites if they are not concentrated at these sites themselves. CpoB still appears to accumulate at constrictions in Δ*tolA* cells (78) but whether this reflects specific localization or is due to the expanded periplasmic volume at these sites in Tol$^-$ cells (23) is unclear. However, even if TolB and CpoB molecules were dispersed throughout the periplasm of TolQAR-minus cells, the expanded periplasmic volume at constriction sites in such cells would cause their numbers to be high at these sites relative to other cell sites. Perhaps weak and transient periplasmic interactions of TolAIII with TolB and CpoB and/or with complexes containing the latter two and Pal drive GFP-M-L-TolAIII toward constriction sites by mass-action. Alternatively, if CpoB does still specifically accumulate at constriction sites in cells lacking functional TolQRA, TolB, and Pal might somehow stimulate or stabilize the TolAIII-CpoB interaction without themselves becoming stably associated with the complex. Another possibility is that TolB, Pal, and CpoB all contribute to the generation or modification of some molecular feature at constriction sites that is attractive to TolAIII but that they are not a stable part of. More work is required to understand the septal localization of GFP-M-L-TolAIII in cells that lack TolQ, TolR, and native TolA. Nevertheless, our results render it likely that all three domains of TolA contribute to its recruitment to, and/or its retention at, constriction sites in wt cells.

Here, we also described the generation and application of functional fluorescent variants of the ZipA division protein that were created by the insertion of RFP or $_{SF}$GFP within its P/Q domain. These sandwich fusions did not display any obvious loss of ZipA functionality, which is concordant with the recent finding that the P/Q domain itself is largely dispensable for ZipA function (110). Availability of these fusions, expressed from the native chromosomal *zipA* locus or ectopically, should be useful for a variety of future studies on the *E. coli* cell division machinery.

MATERIALS AND METHODS

Strains, genetic constructs, and growth conditions. Strains and genetic constructs (plasmids and lysogenic phages) used in this study are listed in Tables S4 and S5, respectively, and their origin or construction is detailed in the supplemental material. Unless stated otherwise, cells were grown at 30°C in LB (1% tryptone, 0.5% yeast extract, 0.5% NaCl, pH = 7.0), LBNS (1% tryptone, 0.5% yeast extract, pH = 7.0), or M9 minimal medium (47.7 mM Na_2HPO_4, 22.0 mM KH_2PO_4, 8.6 mM NaCl, 18.7 mM NH_4Cl, 2.0 mM $MgSO_4$, 0.1 mM CaCl) (111) supplemented with 0.2% Casamino Acids, 50 μg/mL L-tryptophan, 50 μM thiamine, and 0.2% of either maltose (M9-maltose) or glucose (M9-glucose). When appropriate, the medium was supplemented with 50 μg/mL ampicillin (Amp), 25 μg/mL chloramphenicol (Cam), 25 μg/mL kanamycin (Kan), 50 μg/mL spectinomycin (Spec), or 12.5 μg/mL tetracycline (Tet). Amp or Kan concentrations were reduced to 15 and 10 μg/mL, respectively, when cells carried *bla* or *aph* integrated into the chromosome. Arabinose, IPTG (isopropyl-β-D-1-thiogalactopyranoside), and/or aztreonam were included in the media as indicated. Reagents were obtained from Fisher Scientific or MilliporeSigma. Other details are specified in the above.

Microscopy, immunoblotting, and other methods. Imaging was performed on a Zeiss Axioplan-2 microscope system as previously described (8, 112). For some experiments, cells were chemically fixed as described (113) before microscopy. To measure cell dimensions, images were analyzed with Fiji software (114), using the MicrobeJ (115) or ObjectJ (116) plugin as specified in the relevant table captions. No (− −), weak (+ −) or strong (+ +) septal localization of fusion proteins was scored by eye from fluorescent and corresponding DIC images relative to similar images of cells producing GFP-MalF$^{2\text{-}39}$-RodZ$^{139\text{-}255}$, which distributes evenly along the inner membrane (e.g., Fig. 4A and 5A). A subset of representative cells was analyzed with the Fiji Plot Profile function to measure the distribution of signal along a line drawn lengthwise across each cell, and the ratio of peak signal at midcell (septum) and that at the cell pole with the highest signal was determined. Our classification of septal localization corresponded approximately with ratios smaller than 2.1 (no localization), between 2.1 and 2.6 (weak localization), and larger than 2.6 (strong localization). Western blot analyses with anti-GFP antibodies (Rockland) were done essentially as before (106).

SUPPLEMENTAL MATERIAL

Supplemental material is available online only.

SUPPLEMENTAL FILE 1, PDF file, 9.2 MB.

ACKNOWLEDGMENTS

We thank Matthew Gerding, Bing Liu, Felipe Bendezú, Kimberly Girosky, Daniel Bardenstein, Kyle Logue, Christopher Smith, and Thomas Bernhardt for help in plasmid and/or strain construction, and the NCI—Frederick Biological Resources Branch and the Yale Coli Genetic Stock Center for additional strains and plasmids.

This work was supported by NIH grant number GM57059 to PdB.

We declare no conflict of interest.

REFERENCES

1. de Boer PAJ. 2010. Advances in understanding *E. coli* cell fission. Curr Opin Microbiol 13:730–737. https://doi.org/10.1016/j.mib.2010.09.015.
2. Lutkenhaus J, Du S. 2017. *E. coli* cell cycle machinery. Subcell Biochem 84:27–65. https://doi.org/10.1007/978-3-319-53047-5_2.
3. Du S, Lutkenhaus J. 2019. At the heart of bacterial cytokinesis: the Z ring. Trends Microbiol 27:781–791. https://doi.org/10.1016/j.tim.2019.04.011.
4. Bisson-Filho AW, Hsu YP, Squyres GR, Kuru E, Wu F, Jukes C, Sun Y, Dekker C, Holden S, VanNieuwenhze MS, Brun YV, Garner EC. 2017. Treadmilling by FtsZ filaments drives peptidoglycan synthesis and bacterial cell division. Science 355:739–743. https://doi.org/10.1126/science.aak9973.
5. Yang X, Lyu Z, Miguel A, McQuillen R, Huang KC, Xiao J. 2017. GTPase activity-coupled treadmilling of the bacterial tubulin FtsZ organizes septal cell wall synthesis. Science 355:744–747. https://doi.org/10.1126/science.aak9995.
6. Taguchi A, Welsh MA, Marmont LS, Lee W, Sjodt M, Kruse AC, Kahne D, Bernhardt TG, Walker S. 2019. FtsW is a peptidoglycan polymerase that is functional only in complex with its cognate penicillin-binding protein. Nat Microbiol 4:587–594. https://doi.org/10.1038/s41564-018-0345-x.
7. Gerding MA, Liu B, Bendezu FO, Hale CA, Bernhardt TG, de Boer PA. 2009. Self-enhanced accumulation of FtsN at division sites, and roles for other proteins with a SPOR domain (DamX, DedD, and RlpA) in *Escherichia coli* cell constriction. J Bacteriol 191:7383–7401. https://doi.org/10.1128/JB.00811-09.
8. Liu B, Persons L, Lee L, de Boer PA. 2015. Roles for both FtsA and the FtsBLQ subcomplex in FtsN-stimulated cell constriction in *Escherichia coli*. Mol Microbiol 95:945–970. https://doi.org/10.1111/mmi.12906.
9. Tsang MJ, Bernhardt TG. 2015. A role for the FtsQLB complex in cytokinetic ring activation revealed by an *ftsL* allele that accelerates division. Mol Microbiol 95:925–944. https://doi.org/10.1111/mmi.12905.
10. Park KT, Du S, Lutkenhaus J. 2020. Essential role for FtsL in activation of septal peptidoglycan synthesis. mBio 11:e03012-20. https://doi.org/10.1128/mBio.03012-20.
11. Marmont LS, Bernhardt TG. 2020. A conserved subcomplex within the bacterial cytokinetic ring activates cell wall synthesis by the FtsW-FtsI synthase. Proc Natl Acad Sci U S A 117:23879–23885. https://doi.org/10.1073/pnas.2004598117.
12. Liu B, Hale CA, Persons L, Phillips-Mason PJ, de Boer PAJ. 2019. Roles of the DedD Protein in *Escherichia coli* Cell Constriction. J Bacteriol 201:e00698-18. https://doi.org/10.1128/JB.00698-18.
13. Bernard CS, Sadasivam M, Shiomi D, Margolin W. 2007. An altered FtsA can compensate for the loss of essential cell division protein FtsN in *Escherichia coli*. Mol Microbiol 64:1289–1305. https://doi.org/10.1111/j.1365-2958.2007.05738.x.
14. Du S, Pichoff S, Lutkenhaus J. 2016. FtsEX acts on FtsA to regulate divisome assembly and activity. Proc Natl Acad Sci U S A 113:E5052–61. https://doi.org/10.1073/pnas.1606656113.
15. Yang X, McQuillen R, Lyu Z, Phillips-Mason P, De La Cruz A, McCausland JW, Liang H, DeMeester KE, Santiago CC, Grimes CL, de Boer P, Xiao J. 2021. A two-track model for the spatiotemporal coordination of bacterial septal cell wall synthesis revealed by single-molecule imaging of FtsW. Nat Microbiol 6:584–593. https://doi.org/10.1038/s41564-020-00853-0.
16. Egan AJ, Biboy J, van't Veer I, Breukink E, Vollmer W. 2015. Activities and regulation of peptidoglycan synthases. Philos Trans R Soc Lond B Biol Sci 370:20150031. https://doi.org/10.1098/rstb.2015.0031.
17. Cho H, Wivagg CN, Kapoor M, Barry Z, Rohs PD, Suh H, Marto JA, Garner EC, Bernhardt TG. 2016. Bacterial cell wall biogenesis is mediated by SEDS and PBP polymerase families functioning semi-autonomously. Nat Microbiol 1:16172. https://doi.org/10.1038/nmicrobiol.2016.172.
18. Boes A, Olatunji S, Breukink E, Terrak M. 2019. Regulation of the peptidoglycan polymerase activity of PBP1b by antagonist actions of the core divisome proteins FtsBLQ and FtsN. mBio 10:e01912-18. https://doi.org/10.1128/mBio.01912-18.
19. Suzuki H, Nishimura Y, Hirota Y. 1978. On the process of cellular division in *Escherichia coli*: a series of mutants of *E. coli* altered in the penicillin-binding proteins. Proc Natl Acad Sci U S A 75:664–668. https://doi.org/10.1073/pnas.75.2.664.
20. Yousif SY, Broome-Smith JK, Spratt BG. 1985. Lysis of *Escherichia coli* by beta-lactam antibiotics: deletion analysis of the role of penicillin-binding proteins 1A and 1B. J Gen Microbiol 131:2839–2845. https://doi.org/10.1099/00221287-131-10-2839.
21. Pazos M, Peters K, Casanova M, Palacios P, VanNieuwenhze M, Breukink E, Vicente M, Vollmer W. 2018. Z-ring membrane anchors associate with cell wall synthases to initiate bacterial cell division. Nat Commun 9:5090. https://doi.org/10.1038/s41467-018-07559-2.
22. Boes A, Kerff F, Herman R, Touze T, Breukink E, Terrak M. 2020. The bacterial cell division protein fragment (E)FtsN binds to and activates the major peptidoglycan synthase PBP1b. J Biol Chem 295:18256–18265. https://doi.org/10.1074/jbc.RA120.015951.
23. Gerding MA, Ogata Y, Pecora ND, Niki H, de Boer PA. 2007. The trans-envelope Tol-Pal complex is part of the cell division machinery and required for proper outer-membrane invagination during cell constriction in *E. coli*. Mol Microbiol 63:1008–1025. https://doi.org/10.1111/j.1365-2958.2006.05571.x.
24. Yeh YC, Comolli LR, Downing KH, Shapiro L, McAdams HH. 2010. The *Caulobacter* Tol-Pal complex is essential for outer membrane integrity and the positioning of a polar localization factor. J Bacteriol 192:4847–4858. https://doi.org/10.1128/JB.00607-10.
25. Cascales E, Buchanan SK, Duche D, Kleanthous C, Lloubes R, Postle K, Riley M, Slatin S, Cavard D. 2007. Colicin biology. Microbiol Mol Biol Rev 71:158–229. https://doi.org/10.1128/MMBR.00036-06.
26. Szczepaniak J, Press C, Kleanthous C. 2020. The multifarious roles of Tol-Pal in Gram-negative bacteria. FEMS Microbiol Rev 44:490–506. https://doi.org/10.1093/femsre/fuaa018.
27. Parsons LM, Lin F, Orban J. 2006. Peptidoglycan recognition by Pal, an outer membrane lipoprotein. Biochemistry 45:2122–2128. https://doi.org/10.1021/bi052227i.
28. Godlewska R, Wiśniewska K, Pietras Z, Jagusztyn-Krynicka EK. 2009. Peptidoglycan-associated lipoprotein (Pal) of Gram-negative bacteria: function, structure, role in pathogenesis and potential application in immunoprophylaxis. FEMS Microbiol Lett 298:1–11. https://doi.org/10.1111/j.1574-6968.2009.01659.x.
29. Li GW, Burkhardt D, Gross C, Weissman JS. 2014. Quantifying absolute protein synthesis rates reveals principles underlying allocation of cellular resources. Cell 157:624–635. https://doi.org/10.1016/j.cell.2014.02.033.
30. Sturgis JN. 2001. Organisation and evolution of the *tol-pal* gene cluster. J Mol Microbiol Biotechnol 3:113–122.
31. Jacquier N, Viollier PH, Greub G. 2015. The role of peptidoglycan in chlamydial cell division: towards resolving the chlamydial anomaly. FEMS Microbiol Rev 39:262–275. https://doi.org/10.1093/femsre/fuv001.
32. Nichols RJ, Sen S, Choo YJ, Beltrao P, Zietek M, Chaba R, Lee S, Kazmierczak KM, Lee KJ, Wong A, Shales M, Lovett S, Winkler ME, Krogan NJ, Typas A, Gross CA. 2011. Phenotypic landscape of a bacterial cell. Cell 144:143–156. https://doi.org/10.1016/j.cell.2010.11.052.
33. Kowata H, Tochigi S, Kusano T, Kojima S. 2016. Quantitative measurement of the outer membrane permeability in *Escherichia coli lpp* and *tol-pal* mutants defines the significance of Tol-Pal function for maintaining drug resistance. J Antibiot (Tokyo) 69:863–870. https://doi.org/10.1038/ja.2016.50.

34. Shrivastava R, Jiang X, Chng SS. 2017. Outer membrane lipid homeostasis via retrograde phospholipid transport in *Escherichia coli*. Mol Microbiol 106:395–408. https://doi.org/10.1111/mmi.13772.
35. Masilamani R, Cian MB, Dalebroux ZD. 2018. *Salmonella* Tol-Pal reduces outer membrane glycerophospholipid levels for envelope homeostasis and survival during bacteremia. Infect Immun 86:e00173-18. https://doi.org/10.1128/IAI.00173-18.
36. Bernadac A, Gavioli M, Lazzaroni JC, Raina S, Lloubes R. 1998. *Escherichia coli tol-pal* mutants form outer membrane vesicles. J Bacteriol 180:4872–4878. https://doi.org/10.1128/JB.180.18.4872-4878.1998.
37. Meury J, Devilliers G. 1999. Impairment of cell division in *tolA* mutants of *Escherichia coli* at low and high medium osmolarities. Biol Cell 91:67–75. https://doi.org/10.1111/j.1768-322X.1999.tb01085.x.
38. Teleha MA, Miller AC, Larsen RA. 2013. Overexpression of the *Escherichia coli* TolQ protein leads to a null-FtsN-like division phenotype. MicrobiologyOpen 2:618–632. https://doi.org/10.1002/mbo3.101.
39. Tsang MJ, Yakhnina AA, Bernhardt TG. 2017. NlpD links cell wall remodeling and outer membrane invagination during cytokinesis in *Escherichia coli*. PLoS Genet 13:e1006888. https://doi.org/10.1371/journal.pgen.1006888.
40. Petiti M, Serrano B, Faure L, Lloubes R, Mignot T, Duche D. 2019. Tol energy-driven localization of pal and anchoring to the peptidoglycan promote outer-membrane constriction. J Mol Biol 431:3275–3288. https://doi.org/10.1016/j.jmb.2019.05.039.
41. Yakhnina AA, Bernhardt TG. 2020. The Tol-Pal system is required for peptidoglycan-cleaving enzymes to complete bacterial cell division. Proc Natl Acad Sci U S A 117:6777–6783. https://doi.org/10.1073/pnas.1919267117.
42. Cascales E, Gavioli M, Sturgis JN, Lloubes R. 2000. Proton motive force drives the interaction of the inner membrane TolA and outer membrane pal proteins in *Escherichia coli*. Mol Microbiol 38:904–915. https://doi.org/10.1046/j.1365-2958.2000.02190.x.
43. Germon P, Ray MC, Vianney A, Lazzaroni JC. 2001. Energy-dependent conformational change in the TolA protein of *Escherichia coli* involves its N-terminal domain, TolQ, and TolR. J Bacteriol 183:4110–4114. https://doi.org/10.1128/JB.183.14.4110-4114.2001.
44. Goemaere EL, Devert A, Lloubes R, Cascales E. 2007. Movements of the TolR C-terminal domain depend on TolQR ionizable key residues and regulate activity of the Tol complex. J Biol Chem 282:17749–17757. https://doi.org/10.1074/jbc.M701002200.
45. Zhang XY, Goemaere EL, Thome R, Gavioli M, Cascales E, Lloubes R. 2009. Mapping the interactions between *escherichia coli tol* subunits: rotation of the TolR transmembrane helix. J Biol Chem 284:4275–4282. https://doi.org/10.1074/jbc.M805257200.
46. Cascales E, Lloubes R, Sturgis JN. 2001. The TolQ-TolR proteins energize TolA and share homologies with the flagellar motor proteins MotA-MotB. Mol Microbiol 42:795–807. https://doi.org/10.1046/j.1365-2958.2001.02673.x.
47. Zhang XY, Goemaere EL, Seddiki N, Celia H, Gavioli M, Cascales E, Lloubes R. 2011. Mapping the interactions between *Escherichia coli* TolQ transmembrane segments. J Biol Chem 286:11756–11764. https://doi.org/10.1074/jbc.M110.192773.
48. Levengood SK, Beyer WF, Jr., Webster RE. 1991. TolA: a membrane protein involved in colicin uptake contains an extended helical region. Proc Natl Acad Sci U S A 88:5939–5943. https://doi.org/10.1073/pnas.88.14.5939.
49. Derouiche R, Benedetti H, Lazzaroni JC, Lazdunski C, Lloubes R. 1995. Protein complex within *Escherichia coli* inner membrane. TolA N-terminal domain interacts with TolQ and TolR proteins. J Biol Chem 270:11078–11084. https://doi.org/10.1074/jbc.270.19.11078.
50. Germon P, Clavel T, Vianney A, Portalier R, Lazzaroni JC. 1998. Mutational analysis of the *Escherichia coli* K-12 TolA N-terminal region and characterization of its TolQ-interacting domain by genetic suppression. J Bacteriol 180:6433–6439. https://doi.org/10.1128/JB.180.24.6433-6439.1998.
51. Journet L, Rigal A, Lazdunski C, Benedetti H. 1999. Role of TolR N-terminal, central, and C-terminal domains in dimerization and interaction with TolA and tolQ. J Bacteriol 181:4476–4484. https://doi.org/10.1128/JB.181.15.4476-4484.1999.
52. Derouiche R, LloubèS R, Sasso S, Bouteille H, Oughideni R, Lazdunski C, Loret E. 1999. Circular dichroism and molecular modeling of the *E. coli* TolA periplasmic domains. Biospectroscopy 5:189–198. https://doi.org/10.1002/(SICI)1520-6343(1999)5:3<189::AID-BSPY8>3.0.CO;2-O.
53. Witty M, Sanz C, Shah A, Grossmann JG, Mizuguchi K, Perham RN, Luisi B. 2002. Structure of the periplasmic domain of *Pseudomonas aeruginosa* TolA: evidence for an evolutionary relationship with the TonB transporter. protein. EMBO J 21:4207–4218. https://doi.org/10.1093/emboj/cdf417.
54. Lubkowski J, Hennecke F, Pluckthun A, Wlodawer A. 1999. Filamentous phage infection: crystal structure of g3p in complex with its coreceptor, the C-terminal domain of TolA. Structure 7:711–722. https://doi.org/10.1016/s0969-2126(99)80092-6.
55. Deprez C, Lloubes R, Gavioli M, Marion D, Guerlesquin F, Blanchard L. 2005. Solution structure of the *E. coli* TolA C-terminal domain reveals conformational changes upon binding to the phage g3p N-terminal domain. J Mol Biol 346:1047–1057. https://doi.org/10.1016/j.jmb.2004.12.028.
56. Ford CG, Kolappan S, Phan HTH, Waldor MK, Winther-Larsen HC, Craig L. 2012. Crystal Structures of a CTXφ pIII Domain Unbound and in Complex with a *Vibrio cholerae* TolA Domain Reveal Novel Interaction Interfaces. J Biol Chem 287:36258–36272. https://doi.org/10.1074/jbc.M112.403386.
57. Walburger A, Lazdunski C, Corda Y. 2002. The Tol/Pal system function requires an interaction between the C-terminal domain of TolA and the N-terminal domain of TolB. Mol Microbiol 44:695–708. https://doi.org/10.1046/j.1365-2958.2002.02895.x.
58. Bonsor DA, Hecht O, Vankemmelbeke M, Sharma A, Krachler AM, Housden NG, Lilly KJ, James R, Moore GR, Kleanthous C. 2009. Allosteric beta-propeller signalling in TolB and its manipulation by translocating colicins. EMBO J 28:2846–2857. https://doi.org/10.1038/emboj.2009.224.
59. Ridley H, Lakey JH. 2015. Antibacterial toxin colicin N and phage protein G3p compete with TolB for a binding site on TolA. Microbiology (Reading) 161:503–515. https://doi.org/10.1099/mic.0.000024.
60. Szczepaniak J, Holmes P, Rajasekar K, Kaminska R, Samsudin F, Inns PG, Rassam P, Khalid S, Murray SM, Redfield C, Kleanthous C. 2020. The lipoprotein Pal stabilises the bacterial outer membrane during constriction by a mobilisation-and-capture mechanism. Nat Commun 11:1305. https://doi.org/10.1038/s41467-020-15083-5.
61. Nan B, Zusman DR. 2011. Uncovering the mystery of gliding motility in the myxobacteria. Annu Rev Genet 45:21–39. https://doi.org/10.1146/annurev-genet-110410-132547.
62. Wille T, Wagner C, Mittelstadt W, Blank K, Sommer E, Malengo G, Dohler D, Lange A, Sourjik V, Hensel M, Gerlach RG. 2014. SiiA and SiiB are novel type I secretion system subunits controlling SPI4-mediated adhesion of *Salmonella enterica*. Cell Microbiol 16:161–178. https://doi.org/10.1111/cmi.12222.
63. Faure LM, Fiche JB, Espinosa L, Ducret A, Anantharaman V, Luciano J, Lhospice S, Islam ST, Treguier J, Sotes M, Kuru E, Van Nieuwenhze MS, Brun YV, Theodoly O, Aravind L, Nollmann M, Mignot T. 2016. The mechanism of force transmission at bacterial focal adhesion complexes. Nature 539:530–535. https://doi.org/10.1038/nature20121.
64. Cascales E, Lloubes R. 2004. Deletion analyses of the peptidoglycan-associated lipoprotein Pal reveals three independent binding sequences including a TolA box. Mol Microbiol 51:873–885. https://doi.org/10.1046/j.1365-2958.2003.03881.x.
65. Goemaere EL, Cascales E, Lloubes R. 2007. Mutational analyses define helix organization and key residues of a bacterial membrane energy-transducing complex. J Mol Biol 366:1424–1436. https://doi.org/10.1016/j.jmb.2006.12.020.
66. Bouveret E, Derouiche R, Rigal A, Lloubes R, Lazdunski C, Benedetti H. 1995. Peptidoglycan-associated lipoprotein-TolB interaction. A possible key to explaining the formation of contact sites between the inner and outer membranes of *Escherichia coli*. J Biol Chem 270:11071–11077. https://doi.org/10.1074/jbc.270.19.11071.
67. Carr S, Penfold CN, Bamford V, James R, Hemmings AM. 2000. The structure of TolB, an essential component of the *tol*-dependent translocation system, and its protein-protein interaction with the translocation domain of colicin E9. Structure 8:57–66. https://doi.org/10.1016/s0969-2126(00)00079-4.
68. Bouveret E, Benedetti H, Rigal A, Loret E, Lazdunski C. 1999. In vitro characterization of peptidoglycan-associated lipoprotein (PAL)-peptidoglycan and PAL-TolB interactions. J Bacteriol 181:6306–6311. https://doi.org/10.1128/JB.181.20.6306-6311.1999.
69. Bonsor DA, Grishkovskaya I, Dodson EJ, Kleanthous C. 2007. Molecular mimicry enables competitive recruitment by a natively disordered protein. J Am Chem Soc 129:4800–4807. https://doi.org/10.1021/ja070153n.
70. Kleanthous C. 2010. Swimming against the tide: progress and challenges in our understanding of colicin translocation. Nat Rev Microbiol 8:843–848. https://doi.org/10.1038/nrmicro2454.
71. Egan AJF. 2018. Bacterial outer membrane constriction. Mol Microbiol 107:676–687. https://doi.org/10.1111/mmi.13908.

72. Vianney A, Muller MM, Clavel T, Lazzaroni JC, Portalier R, Webster RE. 1996. Characterization of the *tol-pal* region of *Escherichia coli* K-12: translational control of *tolR* expression by TolQ and identification of a new open reading frame downstream of pal encoding a periplasmic protein. J Bacteriol 178:4031–4038. https://doi.org/10.1128/jb.178.14.4031-4038.1996.
73. Sun TP, Webster RE. 1987. Nucleotide sequence of a gene cluster involved in entry of E colicins and single-stranded DNA of infecting filamentous bacteriophages into *Escherichia coli*. J Bacteriol 169:2667–2674. https://doi.org/10.1128/jb.169.6.2667-2674.1987.
74. Gully D, Bouveret E. 2006. A protein network for phospholipid synthesis uncovered by a variant of the tandem affinity purification method in *Escherichia coli*. Proteomics 6:282–293. https://doi.org/10.1002/pmic.200500115.
75. Angelini A, Cendron L, Goncalves S, Zanotti G, Terradot L. 2008. Structural and enzymatic characterization of HP0496, a YbgC thioesterase from *Helicobacter pylori*. Proteins 72:1212–1221. https://doi.org/10.1002/prot.22014.
76. Krachler AM, Sharma A, Cauldwell A, Papadakos G, Kleanthous C. 2010. TolA modulates the oligomeric status of YbgF in the bacterial periplasm. J Mol Biol 403:270–285. https://doi.org/10.1016/j.jmb.2010.08.050.
77. Egan AJF, Maya-Martinez R, Ayala I, Bougault CM, Banzhaf M, Breukink E, Vollmer W, Simorre JP. 2018. Induced conformational changes activate the peptidoglycan synthase PBP1B. Mol Microbiol 110:335–356. https://doi.org/10.1111/mmi.14082.
78. Gray AN, Egan AJ, Van't Veer IL, Verheul J, Colavin A, Koumoutsi A, Biboy J, Altelaar AF, Damen MJ, Huang KC, Simorre JP, Breukink E, den Blaauwen T, Typas A, Gross CA, Vollmer W. 2015. Coordination of peptidoglycan synthesis and outer membrane constriction during *Escherichia coli* cell division. Elife 4:e07118. https://doi.org/10.7554/eLife.07118.
79. Baba T, Ara T, Hasegawa M, Takai Y, Okumura Y, Baba M, Datsenko KA, Tomita M, Wanner BL, Mori H. 2006. Construction of *Escherichia coli* K-12 in-frame, single-gene knockout mutants: the Keio collection. Mol Syst Biol 2:2006.0008. https://doi.org/10.1038/msb4100050.
80. Heilpern AJ, Waldor MK. 2000. CTXphi infection of *Vibrio cholerae* requires the *tolQRA* gene products. J Bacteriol 182:1739–1747. https://doi.org/10.1128/JB.182.6.1739-1747.2000.
81. Llamas MA, Ramos JL, Rodriguez-Herva JJ. 2000. Mutations in each of the tol genes of *Pseudomonas putida* reveal that they are critical for maintenance of outer membrane stability. J Bacteriol 182:4764–4772. https://doi.org/10.1128/JB.182.17.4764-4772.2000.
82. Dubuisson JF, Vianney A, Hugouvieux-Cotte-Pattat N, Lazzaroni JC. 2005. Tol-Pal proteins are critical cell envelope components of *Erwinia chrysanthemi* affecting cell morphology and virulence. Microbiology (Reading) 151:3337–3347. https://doi.org/10.1099/mic.0.28237-0.
83. Lo Sciuto A, Fernandez-Pinar R, Bertuccini L, Iosi F, Superti F, Imperi F. 2014. The periplasmic protein TolB as a potential drug target in *Pseudomonas aeruginosa*. PLoS One 9:e103784. https://doi.org/10.1371/journal.pone.0103784.
84. Gao T, Meng Q, Gao H. 2017. Thioesterase YbgC affects motility by modulating c-di-GMP levels in *Shewanella oneidensis*. Sci Rep 7:3932. https://doi.org/10.1038/s41598-017-04285-5.
85. Santos TM, Lin TY, Rajendran M, Anderson SM, Weibel DB. 2014. Polar localization of *Escherichia coli* chemoreceptors requires an intact Tol-Pal complex. Mol Microbiol 92:985–1004. https://doi.org/10.1111/mmi.12609.
86. Bertsche U, Kast T, Wolf B, Fraipont C, Aarsman ME, Kannenberg K, von Rechenberg M, Nguyen-Disteche M, den Blaauwen T, Holtje JV, Vollmer W. 2006. Interaction between two murein (peptidoglycan) synthases, PBP3 and PBP1B, in *Escherichia coli*. Mol Microbiol 61:675–690. https://doi.org/10.1111/j.1365-2958.2006.05280.x.
87. Typas A, Banzhaf M, van den Berg van Saparoea B, Verheul J, Biboy J, Nichols RJ, Zietek M, Beilharz K, Kannenberg K, von Rechenberg M, Breukink E, den Blaauwen T, Gross CA, Vollmer W. 2010. Regulation of peptidoglycan synthesis by outer-membrane proteins. Cell 143:1097–1109. https://doi.org/10.1016/j.cell.2010.11.038.
88. de Boer PAJ, Crossley RE, Rothfield LI. 1989. A division inhibitor and a topological specificity factor coded for by the minicell locus determine proper placement of the division septum in *E. coli*. Cell 56:641–649. https://doi.org/10.1016/0092-8674(89)90586-2.
89. Oldham ML, Khare D, Quiocho FA, Davidson AL, Chen J. 2007. Crystal structure of a catalytic intermediate of the maltose transporter. Nature 450:515–521. https://doi.org/10.1038/nature06264.
90. Bendezu FO, Hale CA, Bernhardt TG, de Boer PA. 2009. RodZ (YfgA) is required for proper assembly of the MreB actin cytoskeleton and cell shape in *E. coli*. EMBO J 28:193–204. https://doi.org/10.1038/emboj.2008.264.
91. Hale CA, de Boer PAJ. 1997. Direct binding of FtsZ to ZipA, an essential component of the septal ring structure that mediates cell division in *E. coli*. Cell 88:175–185. https://doi.org/10.1016/S0092-8674(00)81838-3.
92. Muller P, Ewers C, Bertsche U, Anstett M, Kallis T, Breukink E, Fraipont C, Terrak M, Nguyen-Disteche M, Vollmer W. 2007. The essential cell division protein FtsN interacts with the murein (peptidoglycan) synthase PBP1B in *Escherichia coli*. J Biol Chem 282:36394–36402. https://doi.org/10.1074/jbc.M706390200.
93. Sykes RB, Bonner DP, Bush K, Georgopapadakou NH. 1982. Azthreonam (SQ 26,776), a synthetic monobactam specifically active against aerobic gram-negative bacteria. Antimicrob Agents Chemother 21:85–92. https://doi.org/10.1128/AAC.21.1.85.
94. Kocaoglu O, Carlson EE. 2015. Profiling of beta-lactam selectivity for penicillin-binding proteins in *Escherichia coli* strain DC2. Antimicrob Agents Chemother 59:2785–2790. https://doi.org/10.1128/AAC.04552-14.
95. Mosyak L, Zhang Y, Glasfeld E, Haney S, Stahl M, Seehra J, Somers WS. 2000. The bacterial cell-division protein ZipA and its interaction with an FtsZ fragment revealed by X-ray crystallography. EMBO J 19:3179–3191. https://doi.org/10.1093/emboj/19.13.3179.
96. Hale CA, de Boer PAJ. 1999. Recruitment of ZipA to the septal ring of *Escherichia coli* is dependent on FtsZ, and independent of FtsA. J Bacteriol 181:167–176. https://doi.org/10.1128/JB.181.1.167-176.1999.
97. Pichoff S, Lutkenhaus J. 2002. Unique and overlapping roles for ZipA and FtsA in septal ring assembly in *Escherichia coli*. EMBO J 21:685–693. https://doi.org/10.1093/emboj/21.4.685.
98. Vega DE, Margolin W. 2019. Direct interaction between the two Z ring membrane anchors FtsA and ZipA. J Bacteriol 201:e00579-18. https://doi.org/10.1128/JB.00579-18.
99. Ohashi T, Hale CA, De Boer PA, Erickson HP. 2002. Structural evidence that the P/Q domain of ZipA is an unstructured, flexible tether between the membrane and the C-Terminal FtsZ-binding domain. J Bacteriol 184:4313–4315. https://doi.org/10.1128/JB.184.15.4313-4315.2002.
100. Hale CA, Rhee AC, de Boer PAJ. 2000. ZipA-induced bundling of FtsZ polymers mediated by an interaction between C-terminal domains. J Bacteriol 182:5153–5166. https://doi.org/10.1128/JB.182.18.5153-5166.2000.
101. Moore DA, Whatley ZN, Joshi CP, Osawa M, Erickson HP. 2017. Probing for binding regions of the FtsZ protein surface through site-directed insertions: discovery of fully functional FtsZ-fluorescent proteins. J Bacteriol 199:e00553-16. https://doi.org/10.1128/JB.00553-16.
102. Warming S, Costantino N, Court DL, Jenkins NA, Copeland NG. 2005. Simple and highly efficient BAC recombineering using *galK* selection. Nucleic Acids Res 33:e36. https://doi.org/10.1093/nar/gni035.
103. Geissler B, Elraheb D, Margolin W. 2003. A gain-of-function mutation in *ftsA* bypasses the requirement for the essential cell division gene *zipA* in *Escherichia coli*. Proc Natl Acad Sci U S A 100:4197–4202. https://doi.org/10.1073/pnas.0635003100.
104. Hale CA, de Boer PAJ. 2002. ZipA is required for recruitment of FtsK, FtsQ, FtsL, and FtsN to the septal ring in *Escherichia coli*. J Bacteriol 184:2552–2556. https://doi.org/10.1128/JB.184.9.2552-2556.2002.
105. Soderstrom B, Mirzadeh K, Toddo S, von Heijne G, Skoglund U, Daley DO. 2016. Coordinated disassembly of the divisome complex in *Escherichia coli*. Mol Microbiol 101:425–438. https://doi.org/10.1111/mmi.13400.
106. Bernhardt TG, de Boer PAJ. 2003. The *Escherichia coli* amidase AmiC is a periplasmic septal ring component exported via the twin-arginine transport pathway. Mol Microbiol 48:1171–1182. https://doi.org/10.1046/j.1365-2958.2003.03511.x.
107. Ovchinnikov S, Kinch L, Park H, Liao Y, Pei J, Kim DE, Kamisetty H, Grishin NV, Baker D. 2015. Large-scale determination of previously unsolved protein structures using evolutionary information. Elife 4:e09248. https://doi.org/10.7554/eLife.09248.
108. Celia H, Botos I, Ni X, Fox T, De Val N, Lloubes R, Jiang J, Buchanan SK. 2019. Cryo-EM structure of the bacterial Ton motor subcomplex ExbB-ExbD provides information on structure and stoichiometry. Commun Biol 2:358. https://doi.org/10.1038/s42003-019-0604-2.
109. Green AG, Elhabashy H, Brock KP, Maddamsetti R, Kohlbacher O, Marks DS. 2021. Large-scale discovery of protein interactions at residue resolution using co-evolution calculated from genomic sequences. Nat Commun 12:1396. https://doi.org/10.1038/s41467-021-21636-z.

110. Schoenemann KM, Vega DE, Margolin W. 2020. Peptide linkers within the essential FtsZ membrane tethers ZipA and FtsA are nonessential for cell division. J Bacteriol 202. https://doi.org/10.1128/JB.00720-19.
111. Roskams J, Rodgers L. 2002. Lab ref: a handbook of recipes, reagents, and other reference tools for use at the bench. Cold Spring Harbor Laboratory Press, Cold Spring Harbor, New York.
112. Johnson JE, Lackner LL, de Boer PAJ. 2002. Targeting of ^{D}MinC/MinD and ^{D}MinC/DicB complexes to septal rings in *Escherichia coli* suggests a multistep mechanism for MinC-mediated destruction of nascent FtsZ-rings. J Bacteriol 184:2951–2962. https://doi.org/10.1128/JB.184.11.2951-2962.2002.
113. Bendezu FO, de Boer PA. 2008. Conditional lethality, division defects, membrane involution, and endocytosis in *mre* and *mrd* shape mutants of *Escherichia coli*. J Bacteriol 190:1792–1811. https://doi.org/10.1128/JB.01322-07.
114. Schindelin J, Arganda-Carreras I, Frise E, Kaynig V, Longair M, Pietzsch T, Preibisch S, Rueden C, Saalfeld S, Schmid B, Tinevez JY, White DJ, Hartenstein V, Eliceiri K, Tomancak P, Cardona A. 2012. Fiji: an open-source platform for biological-image analysis. Nat Methods 9:676–682. https://doi.org/10.1038/nmeth.2019.
115. Ducret A, Quardokus EM, Brun YV. 2016. MicrobeJ, a tool for high throughput bacterial cell detection and quantitative analysis. Nat Microbiol 1:16077. https://doi.org/10.1038/nmicrobiol.2016.77.
116. Vischer NOE, Huls PG, Woldringh CL. 1994. Object-Image: an interactive image analysis program using structured point collection. Binary 6: 160–166.
117. Huerta AM, Collado-Vides J. 2003. Sigma70 promoters in *Escherichia coli*: specific transcription in dense regions of overlapping promoter-like signals. J Mol Biol 333:261–278. https://doi.org/10.1016/j.jmb.2003.07.017.
118. McDonnell AV, Jiang T, Keating AE, Berger B. 2006. Paircoil2: improved prediction of coiled coils from sequence. Bioinformatics 22:356–358. https://doi.org/10.1093/bioinformatics/bti797.